5 Plant growth in an agroforestry system under different small-scale environments

The experiments presented here were carried out at Cienda site in 2004, the first year of the study. Objectives in section 5.1 were to assess small-scale variability of parameters and obtain a detailed characterisation of the situation 'before planting'. Section 5.2 examines plant performance on the same plot in response to spatial heterogeneity.

5.1 Site parameters

Data refer to the ten Cienda subplots described in section 2.5.1 with some reference measurements on the Cienda paired plots. Vegetation and land uses on the respective subplots are summarised in table 11.

Table 11: Vegetation and land uses for Cienda subplots

Subplot	Slope position	Present vegetation and land use before 2004
1 and 2	Lower	Young secondary forest, mainly *Ficus spp.;* coconut
3	Middle	
4	Upper middle	
5	Middle	
6 and 7	Lower	Open fallow dominated by *Imperata sp.*; coconut
8	Middle	Banana and coconut
9	Middle	Fallow dominated by *Pueraria sp.* and grasses; coconut; cassava until 2003
10	Upper middle	Young secondary forest, mainly *Ficus spp.;* coconut
11 and 13	Plateau	Rainforestation; coconut (extensive use for palm wine)
12	Plateau	Fallow dominated by grasses and bush; coconut; previously annual crops

Subplots 1 to 5 and 6 to 10 belong to two different owners and land use was more intensive for the last 10-15 years on subplots 6-10. Subplots 11-13 are located on a plateau approximately 500m away as described in chapter 3 as dystric Nitisol and in chapter 4 as Cienda RF / grassland. Cocos palms are planted randomly across all subplots in distances of 10x10 to 15x15m.

5.1.1 Soil organic carbon (C_{org})

Responding relatively quickly to management or land use change, soil organic matter was expected to be a sensitive indicator for small-scale variability. 20 auger samples from 0-5 and 7-12cm depths each (Ah and AB horizons) were taken in a systematic pattern[68] in each of the 10 subplots and soil organic matter (SOM) was determined by Loss on Ignition method. Values of C_{org} were calculated on the basis of LoI and clay contents according to the regression given in 2.5.13.4. Fig.53 gives an overview of magnitudes and dispersion of the data. Variability within subplots was lower than expected: Coefficients of variation ranged between 8 and 16% at 0-5cm and 5 – 15% at 7-12cm depth.

---

68 i.e. in an equidistant grid with every sampling point referenced

_C__{org} 0-5cm Cienda subplots   **_C__{org} 7-12cm Cienda subplots**
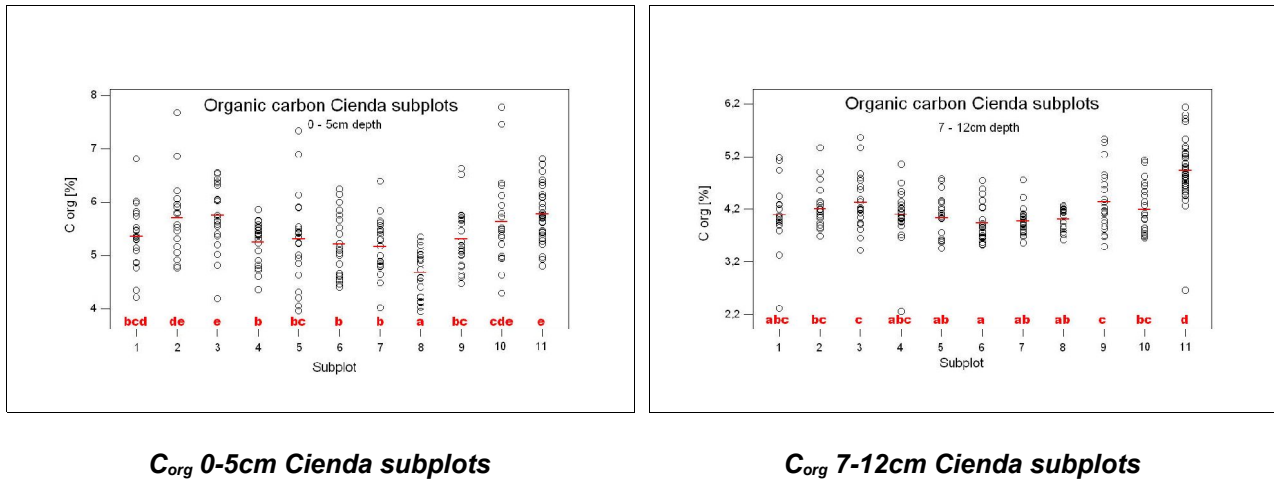
Figure 53: Contents and small-scale heterogeneity of organic carbon contents 0-5cm and 7-12cm at Cienda subplots. Note different scales. Letters a-e indicate homogeneous groups based on Waller-Duncan statistics – same letters belong to same groups

Identical letters group subplots, that did not differ significantly (α <0.05) from each other in a one-way ANOVA applying the Waller-Duncan post-hoc test. As not all subplot values were normally distributed at 7-12cm[69] depth, the non-parametric Mann-Whitney test was additionally applied on this set. This test is more conservative than the t-test-based Waller-Duncan statistics, but resulted in a very similar grouping.

At 0-5cm, the eroded banana subplot 8 was clearly lowest in C_{org}, followed by a group that contained the open grassland area 6 and 7, a subplot previously planted to rootcrops (9), and to middle slope positions under canopy (4 and 5). Subplot 2, 3 and 10 at the upper end of scale came close to the old rainforestation demo site 11.

For 7-12cm depth, differences were less pronounced, basically segregating 1-5, 9 and 10 on one hand from 6, 7 and 8 on the other and subplot 11 forming a distinct class. Subplot 8 ranked better than in the top horizon, suggesting that loss of OM was a recent development caused by erosion under the banana plantation. This was affirmed, when a $C_{AB}:C_{Ah}$ - ratio was calculated: Values in all subplots were constricted to tight bounds between 0.74 and 0.78 to the exception of subplots 8, where the Ah was supposedly depleted by erosion (0.86), 9, which had been recently disturbed through harvest of root crops (0.82) and 11, an advanced succession characterised by accumulation of OM (0.85).

The most relevant driver for C_{org} balances was land use, determining vegetation type and management intensity. These, in turn, affect canopy cover and litter inputs. Under grassland and banana, C_{org} was lowest, increasing with more extensive use and standing biomass, e.g. in subplots 3, 10 and 11. Consequently, the 10 year old reforestation showed the highest C_{org} contents of all subplots.

In context with chapter 4, C_{org} values converted from LoI still overestimated those measured directly by EA. This became obvious from subplot 11 aka Cienda rainforestation plot.

---

69 They were for 0-5cm, and variance was homogeneous for both depths.

5.1.2 SOM pools derived by physical fractionation

Different fractions of organic matter have different turnover times in soil (BURESH 1999) and reflect litter quality (CADISCH ET AL. 1996). These fractions can be segregated by a combined size-density fractionation. As an order of magnitude, BALESDENT (1996) calculated turnover times of 0.5 years for the OM fraction >2000µm and 63 years for the fraction <50µm in French Eutric Cambisols. Turnover determines release of nutrients but also structural functions of SOM. For modelling, active, slow and passive SOM fractions are often distinguished by physical methods (for an overview, s. PAUSTIAN ET AL. 1997B). The combined sieve and density fractionation used here (based on ANDERSON & INGRAM 1993 and GAISER 1993) is in accordance with requirements for the CENTURY SOM module on which WaNuLCAS is based[70].

Following the definition of TSBF (ANDERSON & INGRAM 1993), the active pool contains microbial carbon and OM floating on water, the slow pool comprises non-floating OM of 0.25-2mm in size and the passive pool OM of high density (>1.6g/cm^3) smaller 0.25mm. In modification, fractions separated here were AGB >2mm, roots >2mm, charcoal >2mm, light organic matter floating on water (not tungstate) <2mm (LOM) and heavy organic matter <2mm (HOM). Each fraction was weighed and analysed for C, N and P. As a control, the unfractionated sample was analysed for C, N and P, too. Twelve samples were bulked to one composite sample per subplot.

Organic matter fractions *by weight* were dominated by over 98% heavy fraction, which contains all mineral compounds (fig.54). The LOM fraction paralleled results for C$_{org}$, namely low contents at subplots 6-8 and high values at 2, 3, 10 and 11.
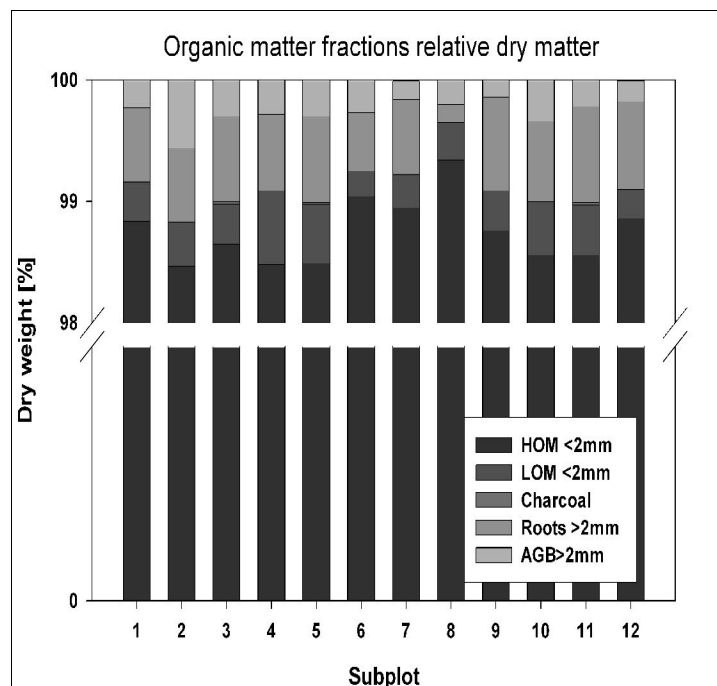

Figure 54: Percentage mass of soil fractions per subplot

Absolute contents of C, N and P as distributed over the various fractions are shown in fig. 55-57.

---

[70] Where the active (mainly C$_{mic}$), the slow or light fraction (0.25-2mm and <0.9gcm^{-3}) and the passive fraction (>1.6gcm^{-3}) are distinguished. As chemical criteria, polyphenolics and lignin contents enter into the WaNuLCAS model.
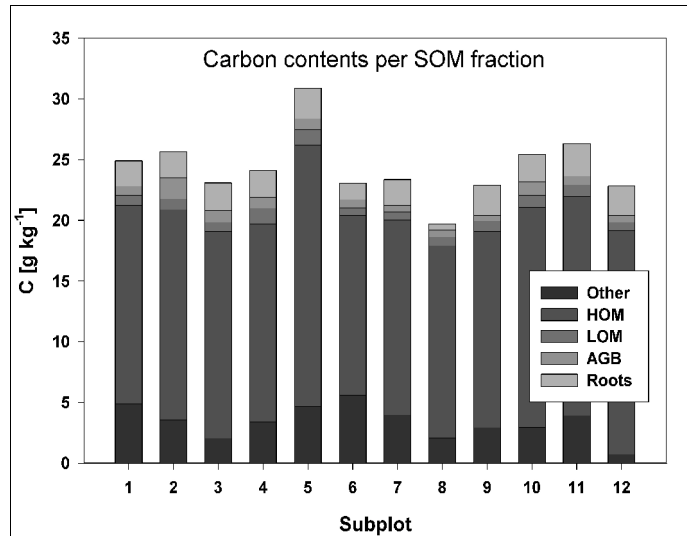
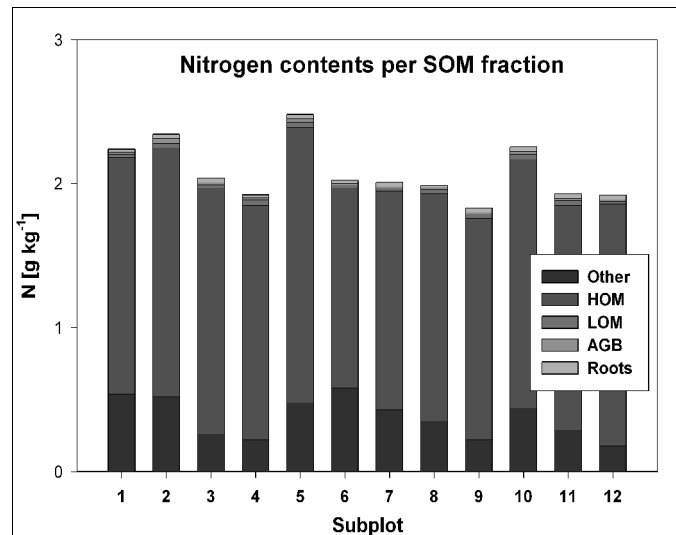**Figure 55: Absolute C contents per fraction and plot**

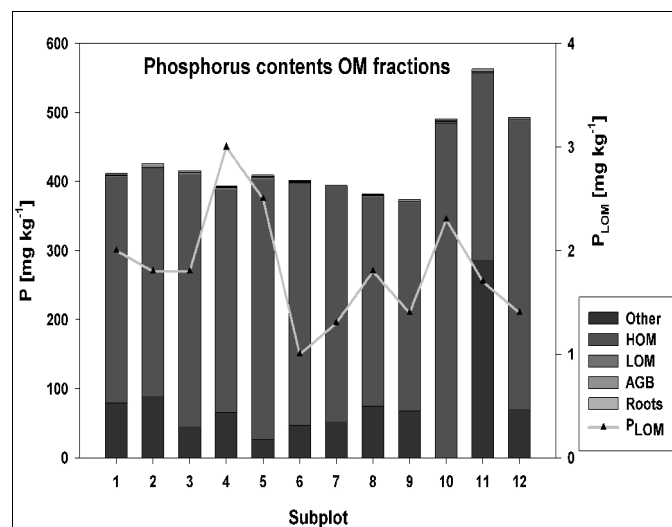**Figure 56: Absolute N contents per fraction and plot**

Figure 57: Absolute P contents per fraction and plot; P_{LOM} highlighted as line

Subplots did not differ much in total C contents, but the very low values at subplot 8, as well as high contents at 2, 10 and 11 are parallel to the findings for C_{org}. Assuming a bulk density of 0.9g cm^{-3} and average C_{LOM} of 0.87g kg^{-1} (see fig.55 for absolute C contents), the sampled top 15cm of the soil contain 1500kg of C_{LOM} ha^{-1}.

As for C, the bulk of N and P was bound to the HOM fraction. Total N and P supply was lowest on subplots 4, 8 and 9. C was by far lowest on 8, as found before (5.1.1). A group of five subplots was generally best supplied: Number 10 with respect to C, N and P, further 1, 2 and 5 for C and N and 11, 12 for C and P. Low P at subplot 4 seems to contradict the good supply of the Ah horizon at nearby profile PN1; as at Marcos site, P seems to be unequally distributed on a small scale. For subplot 10 and 11, 'other' P was suspiciously low / high[71] and data need to be interpreted cautiously.

Carbon contents in the unfractionated samples are below those obtained by EA in the respective profiles (chapter 3) and by LoI in 5.1.1. The fractions in fig. 54-56 denominated *other* refer to the control entire – sum of fractions (16-18% in average). These losses include dissolved organic matter (DOM) containing DOC, DON and DOP, microbial biomass and minor amounts of C and N through the wet sieving process, respiration or denitrification during storage in the pails. The rest was due to the procedure and to charcoal, which was not analysed for C, N, P separately. MAGID ET AL. (2002) allotted charcoal to the water-flotable fraction.

In terms of amounts, BALESDENT (1996) evaluated several methods of fractionation and quantified C fractions for modelling with a wet sieving procedure similar to the one discussed here. In his experiments, *water-soluble C obtained from particle-size fractionation accounted for approximately 1.5% of soil C*. Microbial biomass can make up for 2-7% of C_{org} (INSAM & DOMSCH 1988).

---

71 possibly an analytical error

C:N and C:P-ratios (fig. 58 and 59) give information on decomposability of substrates, tight ratios indicating better access for microbial decomposers.
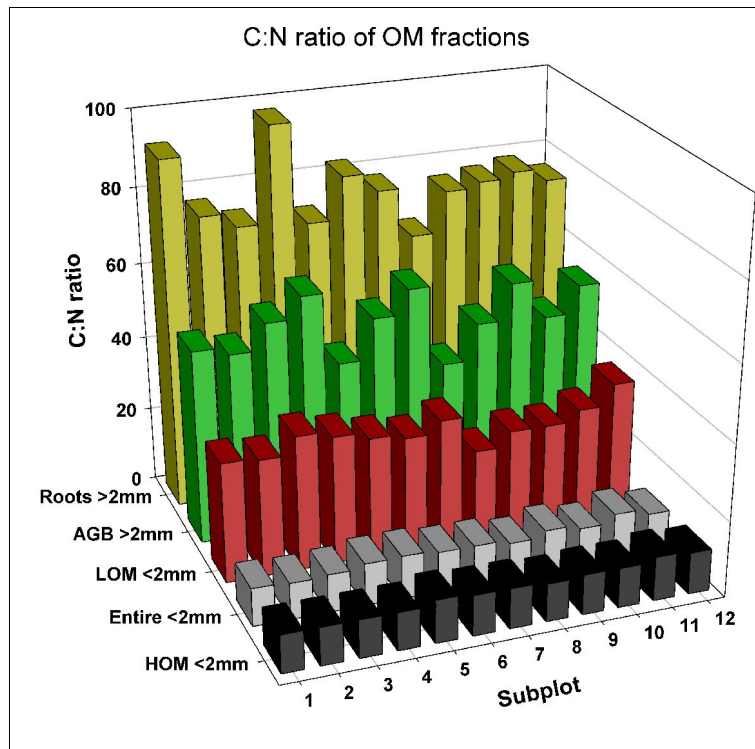

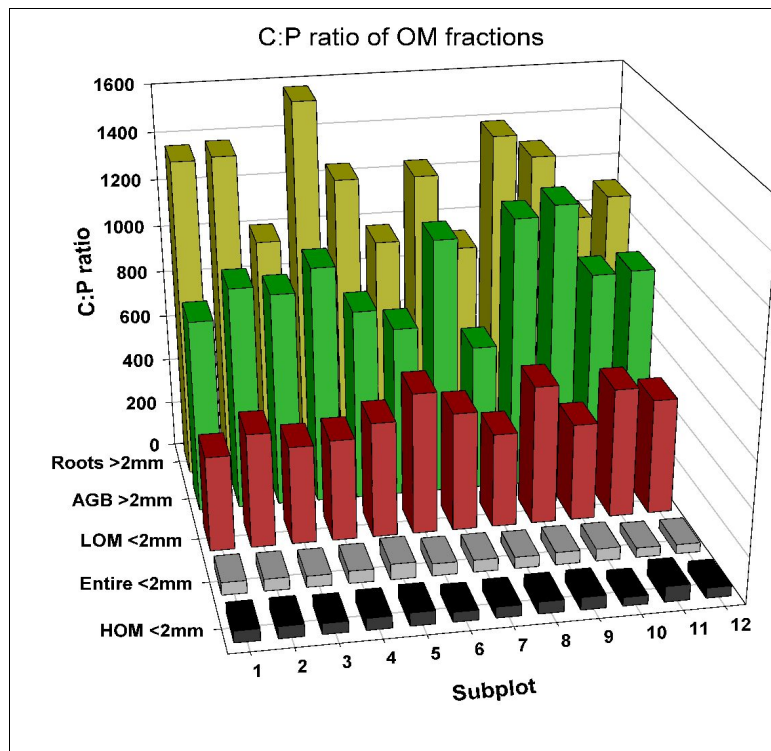**Figure 58: C:N ratios of SOM fractions on Cienda subplots**

Figure 59: C:P ratios of SOM fractions on Cienda subplots

Generally, lighter (and here also larger) fractions show the wider C:N and C:P ratios (GREGORICH ET AL. 1994). Despite its tight C:N- and C:P-ratio, HOM is the most recalcitrant fraction and most difficult to access for microorganisms due to pore size and chemical protection of OM (LAVELLE & SPAIN 2005, FELLER & BEARE 1997). Range of C:N in entire samples was 9.5 to 12.2, consistent with values found in Leyte profiles (chapter 3). C:P-ratios in Cienda subplots were between 41 and 68, which is tight compared to 'typical' levels for tropical agricultural soils (ZECH ET AL. 1997).

Cross-relations between all fractions and subplots cannot be discussed here, but two extremes shall be presented. The tightest C:N and C:P ratios were found on subplot 8 throughout all fractions except for C:P-HOM. If tightening of ratios is an indicator for nutrient accumulation through illuviation (SCHOENAU & BETTANY 1987) or input of litter, this would mean, that easily decomposable banana leaves or stronger leaching or erosion of C compared to P had caused the relative increase. Light organic matter decomposes faster than the heavy organic matter fraction bound to minerals and protected from microbial attack (LAVELLE & SPAIN 2005). The fact, that C:P-HOM as the least changing fraction remained elevated, supports the first assumption of agricultural intensification[72]. The opposite process took place at number 4 with respect to C:N-ratios. This subplot had been managed extensively during the last decade and C:N-ratios in the large and light fractions were among the widest. C:N-HOM, however was among the tightest, along with 1-3 and 8. GAISER (1993) found for maize grown in Benin, that the effect of LOM on maize yields doubled that of HOM. LOM is the most readily available fraction and would be of most significance for planting, while HOM stands for nutrient reserves stored in the soil, but not necessarily accessible in the short run. In table 12 the share of LOM in the entire sample was calculated.

---

[72] Still, tight C:N or C:P does not imply sufficient supply of a nutrient, as in the case of subplot 8 P_{Bray} was comparably low.

Table 12: Shares of C_{LOM}, N_{LOM} and P_{LOM} in element contents of the unfractionated (entire) samples

Subplot	Share of C_{LOM} [%]	Share of N_{LOM} [%]	Share of P_{LOM} [%]
1	18.1	3.66	1.32
2	21.5	5.03	1.54
3	18.9	3.90	1.37
4	21.3	4.44	1.60
5	17.8	4.79	1.47
6	15.0	3.37	0.93
7	17.1	3.58	1.02
8	10.1	3.23	1.05
9	18.9	4.53	1.17
10	19.3	4.61	1.01
11	19.5	4.95	1.85
12	16.5	3.51	0.98

A ranking of these parameters shows, that subplots, which were advanced in succession and produced most litter (5.1.5), e.g. 4, 10[73] and 11, mostly lead with respect to readily available elements. The ones most behind are the eroded banana plot 8, grassland 6&7 and the young bush fallow 12. Contents in C, N and P depend on the plant species, that produce the litter. When subplots are ranked by absolute LOM dry matter, subplots 2 and 8 with their extreme values of $\%N_{LOM}$ and $\%P_{LOM}$ move to the midfield. For subplot 2 this means, that biomass is relatively rich in N and P, whereas banana biomass is low in the analysed elements.

5.1.3 Soil and basal respiration

5.1.3.1 Simultaneous experiment of soil and basal respiration

Soil respiration refers to CO_2 evolution of all biota in the entire soil profile under natural conditions, while basal respiration is usually determined in a sieved sample without roots under standardised laboratory temperature and moisture. Roughly $^2/_3$ of soil respiration are ascribed to microorganisms, the rest to animals and roots (SCHACHTSCHABEL ET AL. 1992). Absolute magnitudes of CO_2 evolved during both experiments cannot be directly related because of the different units (CO_2 per g soil for BR vs. CO_2 per square centimetre for soil respiration) and organisms involved, but relative magnitudes between subplots can be compared. For a simultaneous soil respiration – BR experiment, water contents of BR samples were not adjusted. No rain fell from three days before until the end of the experiments and temperatures were recorded. Fig.66 (section 5.1.6) shows soil temperatures in 5cm depth under closed canopy and grassland. In fig.60, soil temperatures during the experiment were monitored in and outside the pails used for soil respiration.
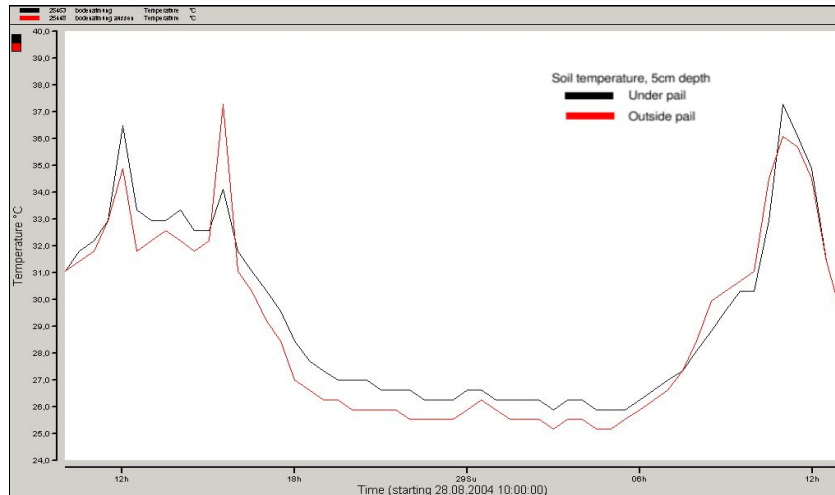
---

73 except P

Figure 60: Soil temperatures (5cm depth) in and outside pails in subplot 1 during the soil respiration experiment

Pails heated up relative to ambient temperatures during midday and kept a more balanced temperature, when the soil outside was warmed by oblique sun rays during late afternoon. Under isothermic conditions as in Leyte soils, the major influence on soil and basal repiration was expected to depend on soil moisture (HASHIMOTO ET AL. 2004). As discussed by DILLY (2001), incubation was at room temperature and natural water contents for better comparison with soil respiration values.
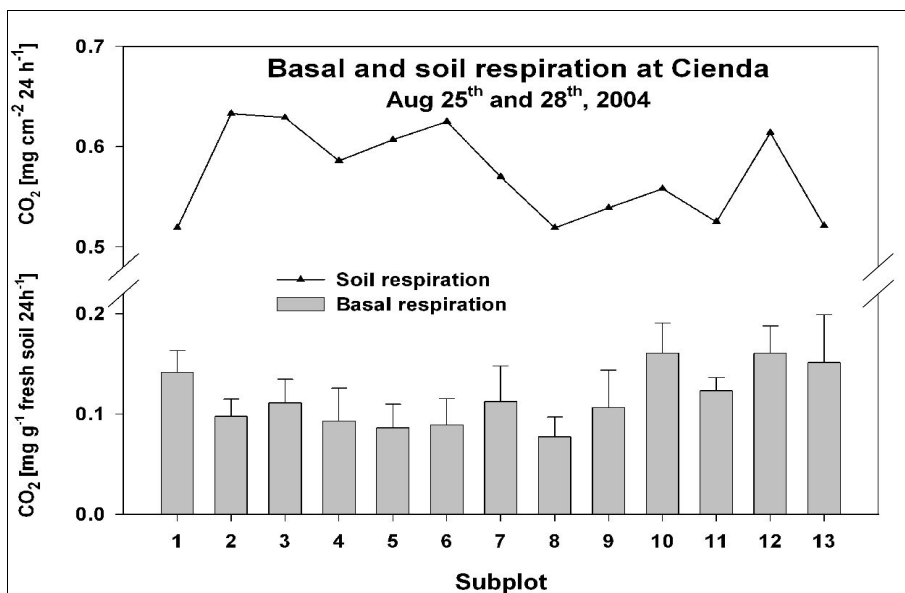

Figure 61: Basal and soil respiration at Cienda (25th and 28th -29th of Aug, 2004), BR at natural water contents. Soil respiration shown as means of two independent samples, BR as means of sevenfold technical replicates of one composite sample per subplot

Fig.61 shows that trends between subplots in both trials differ substantially for subplots 1, 2 and 6, but generally follow the same tendency. Temperature effects may have led to overestimation of soil respiration in the open plots 6, 7 and 12. Subplots 1&2 and 6&7 as adjacent subplots showed considerable differences in CO_2 release for both methods, pointing to high small-scale variability; adjacent 11&13 did not. Higher numbers of replicates might have been necessary to achieve better accuracy, but at the cost of considerable disturbance of the area.

Extrapolating the evaluation curve for soil respiration provided by SCHLICHTING ET AL. (1995; p.254) to an average soil temperature of 29-30°C, all measured values would be classified as *moderate*.

Typical CO_2 effluxes found by SCHWENDENMANN (2002) in Costa Rica were in the order of 0.88-1.76mg CO_2 cm^{-2} d^{-1}(or 100-200mg CO_2-C m^{-2} h^{-1}). Levels found in this study are lower, but comparable to those findings, especially if the deeper solum of the mesoamerican soils is taken into account. RAICH ET AL. (2003) modelled a yearly average release of CO_2-C for Philippine terrestrial soils of >1400gCm^{-2} a^{-1} from 1980-1994 compared to about 600Cm^{-2} a^{-1} in this experiment, assuming a value of 0.6mgCO_2cm^{-2} d^{-1}.

5.1.3.2 'Long-term' basal respiration

For a basal respiration experiment of 30 days duration, 12 samples per subplot were bulked and repeated in seven-fold technical replicate. Since BR depends strongly on water contents (LUIZÃO ET AL. 1992) samples were adjusted to 55% of water holding capacity (WHC) and monitored during the experiment, but evaporation losses found negligible.
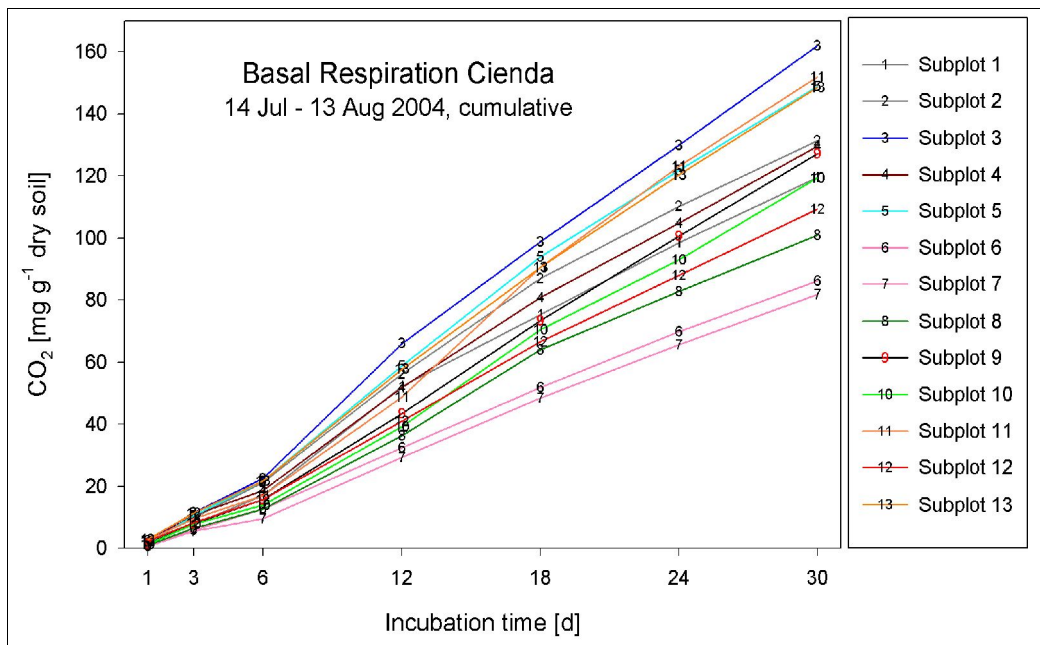

Figure 62: Basal respiration during a 30-day experiment in cumulative depiction

All subplots under canopy were concentrated in the upper half of the graph in fig.62. Subplot 3, under canopy, but prone to erosion, ranks first. Lowest respiration rates were observed in the open areas in subplots 6, 7 and 12 as well as the eroded banana subplot 8. On the other hand, BR also depends on the population size of respiring microorganisms. This can be observed for subplot 9, where elevated BR coincides with an exceptionally large microbial population (s. next section). This large microbial pool may have been caused by disturbance (harvest of cassava in 2003) which led to increased aeration, decomposition and build-up of microbial biomass until a new steady state was to be reached (INSAM & DOMSCH 1988). Contrary to this, low basal respiration for subplots 6 - 8 must be seen in the context of their small microbial population.

Trends of cumulative respiration remained stable during the entire period. Values of adjacent subplots 1&2 were close and parallel throughout the entire incubation period, 6&7 and 11&13 almost identical.

BR on an hourly basis is shown in fig.63 for better comparability with references from literature.

5.1.4 Microbial carbon

As mentioned, the conversion factor suggested by ANDERSON & DOMSCH[74] (1978) for substrate-induced respiration (SIR) is only valid, if the procedure is carried out at 22°C. This requirement could not be met in 2004. In literature, conversion factors given (BECK ET AL. 1997) are for temperatures from 25-28°C or the original factor is used for 25°C (ANDERSSON ET AL. 2004), but not for 32°C, as in the experiment presented here. Consequently, qCO_2 and C_{mic}/C_{org} ratio were calculated on the basis of released CO_2 instead of C_{mic}.

Twenty samples per subplot were bulked and repeated in fivefold technical replicate. Substrate-induced respiration was compared to hourly BR values calculated from the experiment presented in 5.1.3. Basal respiration in fig.63 is displayed on an hourly basis during different periods of a 30-day experiment (e.g. *BR 24d* is the CO_2 released per hour during the period from day 18 to 24).
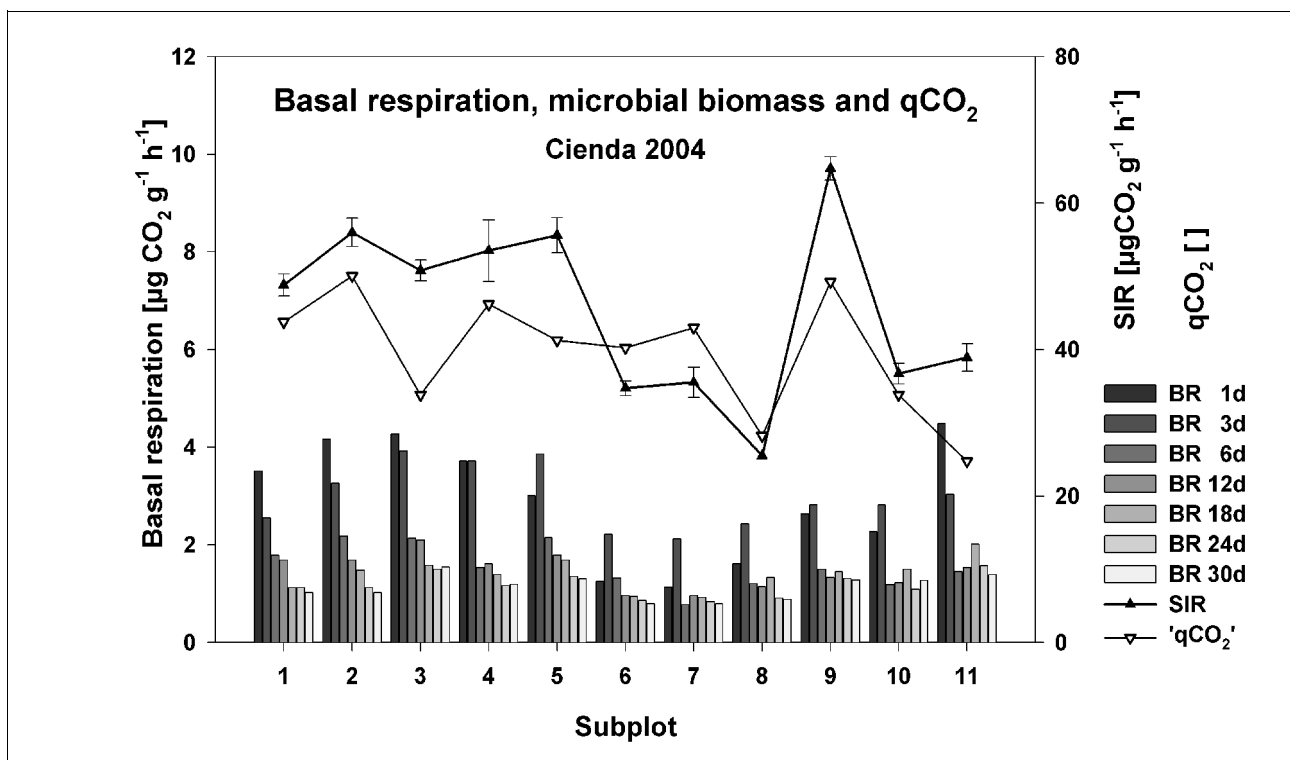

Figure 63: Basal and substrate-induced respiration and qCO_2 on Cienda subplots 2004. All values given on CO_2-basis. qCO_2 refers to BR 24d.

For all subplots, BR started at a high level from day 1 to 3, probably caused by disturbance and aeration of the soil, when samples are mixed and filled into the nylon bags (see MAMILOV & DILLY (2002) about importance of drying-rewetting cycles for microbial respiration). By the time a relative equilibrium was reached, which varied to some degree depending on ambient temperature. The decline of BR in laboratory experiments would continue beyond the 30 days; this is normal and due to depletion of reserves, which are otherwise constantly supplied on site (ANDERSON 1994; FANG ET AL. 2005). SIR is shown as

---

74 C_{mic} [mg 100g^{-1} dry soil] = 20.6 CO_2 [mg 100g^{-1} dry soil h^{-1}] (SCHINNER ET AL. 1993). Originally C_{mic} [mg 100g^{-1} dry soil] = 40x + 0.37, where x is CO_2 [ml 100g^{-1} dry soil h^{-1}].

evolution of CO_2 to circumvent the conversion factor. Both basal respiration and SIR are well distinguishable between land uses, with subplots 1-5 (canopy) on a higher level than 6-10 (open area and banana) and subplot 11 (old rainforestation demo plot) in between. An exception to this overall trend is the low SIR of subplot 8, likely to be caused by erosion of topsoil, which contains most microbial biomass. Subplot 9 is in the stage of a population build-up after disturbance caused by cassava harvest.

qCO_2 is given as BR-24d-CO_2 per SIR-CO_2 instead of the usual BR per unit C_{mic}. *BR 24d* - values were used as they represented an equilibrium state of respiration (ANDERSON & DOMSCH 1986), SIR-CO_2 due to lack of a calibrated conversion factor. With qCO_2 understood as a stressor (s. 4.5), it could be expected, that an undisturbed area under extensive land use like subplot 11, would show low levels and open areas with temporal water stress, 6 and 7, relatively high values. Subplots 8 and 9 are influenced by the factors underlying SIR, namely erosion and post-disturbance.

An overview of C_{mic} and C_{org} as well as the quotient of both is shown in tab.13. This quotient has been suggested as a sensitive indicator for soil fertility and correlated to crop yields (KAISER ET AL. 1992), which reacts quickly to land use or management changes and varies within a range of 0.27 – 7% typical for European soils (ANDERSON & DOMSCH 1989). MAO ET AL. (1992) found typical values 1.2-1.9 for reforested plots and of 1.0 – 1.2 for rainforest in tropical China. For the sampled soils, the original formula by ANDERSON & DOMSCH (1978) was used as an approximation to convert SIR-CO_2 into C_{mic}. Values for C_{mic} and C_{mic}/C_{org} are meant as relative, not as absolute figures to be compared to literature values.

Table 13: Contents of C_{org}, C_{mic} per subplot and C_{mic} as percentage of C_{org}

Subplot	C_{mic} A&D[75]	C_{org} (Ø 0-5 and 7-12cm)	C_{mic} / C_{org}
	[mg g^{-1} soil]	[%]	[% of C_{org}]
1	1.01	4.73	2.13
2	1.15	4.96	2.33
3	1.05	5.04	2.08
4	1.10	4.67	2.36
5	1.15	4.67	2.46
6	0.72	4.57	1.56
7	0.73	4.57	1.60
8	0.53	4.34	1.21
9	1.33	4.82	2.76
10	0.76	4.92	1.54
11	0.80	5.36	1.50

A clear divide between C_{mic}/C_{org} of subplots 1-5 and 6-10 is owed to the higher C_{mic} contents in the first cluster. The recent disturbance of subplot 9 (harvest of cassava in 2003) was reflected by the exceptionally high C_{mic} contents, that overcompensate high C_{org}. Despite its low C_{org} and due to the even lower C_{mic}, subplot 8 ranks last in C_{mic}/C_{org}. As C_{mic} precedes C_{org} in its reaction to land use change, a comparatively high C_{mic}/C_{org}

---

[75] After ANDERSON & DOMSCH (1978): 1mgCO_2g^{-1}soil h^{-1} = 20.6mgC_{mic}g^{-1}soil, if the respiration coefficient is assumed to be 1 (used for 22°C).

quotient is a sign of microbial biomass build-up in progress as in subplot 9 and vice versa for subplot 8.

According to DINESH ET AL. (2004), the quotient C_{mic}/C_{org} reflects substrate availability, with low values indicating recalcitrant substrate. For the examples shown here, C_{mic}/C_{org} reflects the unfavourable conditions at subplots 6-8 and the land use change at 9 well. This agrees with findings by INSAM & DOMSCH (1988), that C_{mic} precedes C_{org} in its reaction to land use changes. Following this logic, subplot 11 can be interpreted as advanced succession characterised by humus accumulation and adaptation of the microbial biomass to (unfavourable because acidic etc.) ambient conditions.

5.1.5 Litter production

Litter production was monitored in order to characterise plot variability in canopy cover and organic matter cycling. While the latter is generally desirable for plant production, the first can stand for protection, but also competition for light or indicator of nutrient or water competition. Three fractions of aboveground litter were distinguished, namely leaves, flowers & fruit (F&F) and bark & branches (B&B). *Leaves* was an interesting category with respect to shedding during dry season and changing understorey light regime. Lignified B&B fraction was considered relevant because of slower decomposition rates and F&F in context with reproductive phenology. Litter of all fractions by subplot is shown in fig.64 for the period Jan 2005 – Jan 2006.
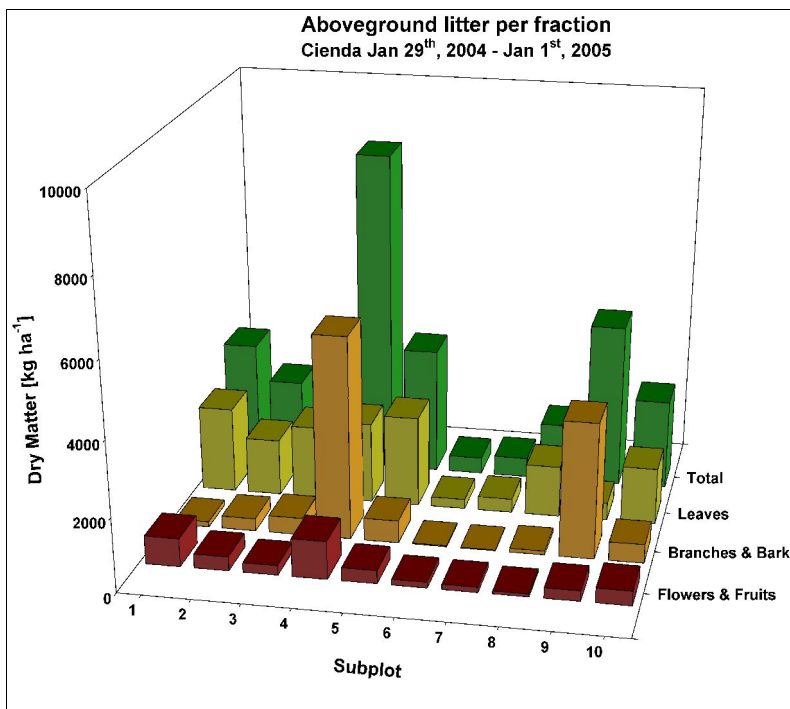

Figure 64: Litter fractions (oven-dry) per subplot in Cienda. Samples collected from Jan 29th, 2005, to Jan 1st, 2006

Leaf litter was identified as the fraction with least dispersion, while F&F and B&B data were distorted by outliers for some subplots. Adding up leaf litter inputs of the entire observation period (Jan 05 – Jan 06), tenure and past land use can be clearly distinguished: Subplots 1-5 under closed canopy differ from 6 and 7 under low-growing *Imperata sp.*, *Saccharum spontaneum* and ferns and subplot 9 (as 6 and 7 plus creepers and scattered small bushes). Subplot 8 is mid-slope banana land and influenced by the more forest-like area around subplot 10 at the upper slope. Total AGB litter follows the same tendencies to the exception of subplot 9, where one coconut stalk distorted the otherwise low overall amounts of B&B.

The presented amounts cover litterfall during a span of 337 days. Extrapolating this to one year time, total aboveground litter is 471 to 9,340kg $ha^{-1}a^{-1}$, in the upper third of what KELLMAN (1970) calculated for secondary forests in Mindanao (2,000-12,000kg litter $ha^{-1}a^{-1}$). ASIO (1996) cites literature data by CUEVAS & SAJISE (1978) of 13.48t litterfall $ha^{-1}a^{-1}$ for a rainforest on volcanic soil at Mt. Makiling, Luzon.
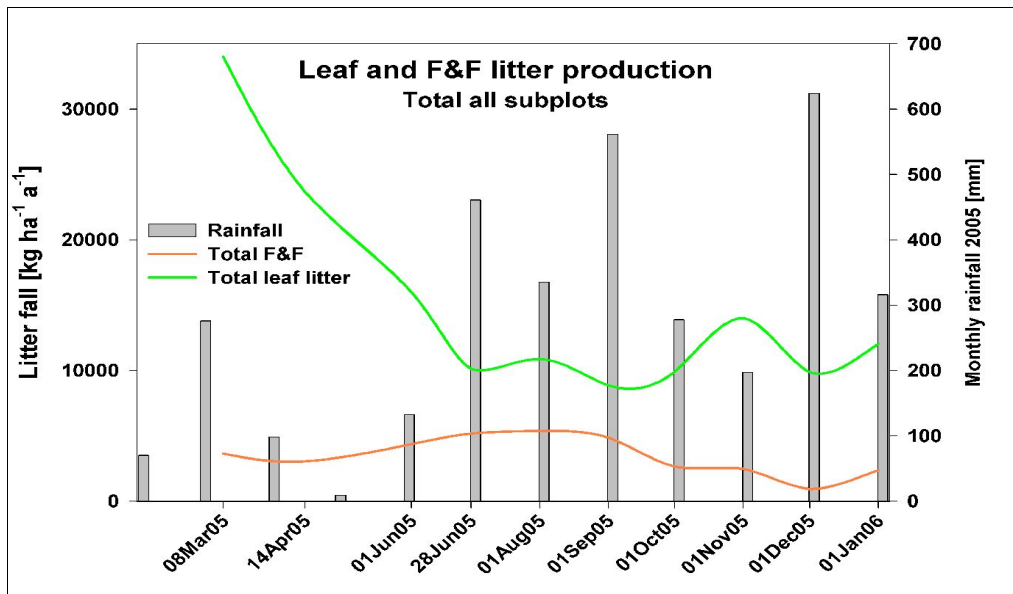
Figure 65: Total leaf and fruit litter time series Cienda

Looking at the temporal distribution of total leaf and F&F litter quantities (fig.65), a maximum of leaf fall was observed for all subplots except 6, 7 and 9 in March 2005 following a dry February. A smaller peak occurred in November, caused by subplots 1 and 4. Between these two peaks a maximum in F&F litter occurred at the end of June to the end of August, which could be observed in most subplots (plotwise data not shown). A background 'noise' of coconut flowers was found throughout the year for all plots including 6, 7 and 9. Outliers on subplots 1 and 4 were caused by aborted coconuts.

5.1.6 Litter decomposition

According to a hierarchical model of factors steering decomposition, soil temperature and moisture are the most powerful drivers, usually outweighing influences exercised by the type of clay minerals, substrate quality and predation of bacteria by protozoa and other organisms (LAVELLE ET AL. 1993).
Soil temperature and water regime differed between subplots depending on canopy cover. As an example, maximum soil temperature (in 5cm depth) during the leaf decomposition experiment in Cienda was >38°C in open areas like subplots 6 and 7 and <31°C for subplots 1, 2 and the rainforestation demo plot installed in 1996 (fig.66).
Clay minerals were not expected to differ strongly, but clay contents did (see sections 3.2.1-4): For subplots 4 and 8 (middle slope) 35-40%, for 6 (footslope) clay contents of 45-50% and for the rainforestation plot ('demo site') of 65-70% were found in the topsoil. Litter quality was controlled by a standard substrate and the role of arthropods and other mesofauna for litter decomposition (directly or through predation on microorganisms) was assessed by net tissue of different mesh width (0.1 and 4mm) allowing access to the litter sample for different decomposer groups.
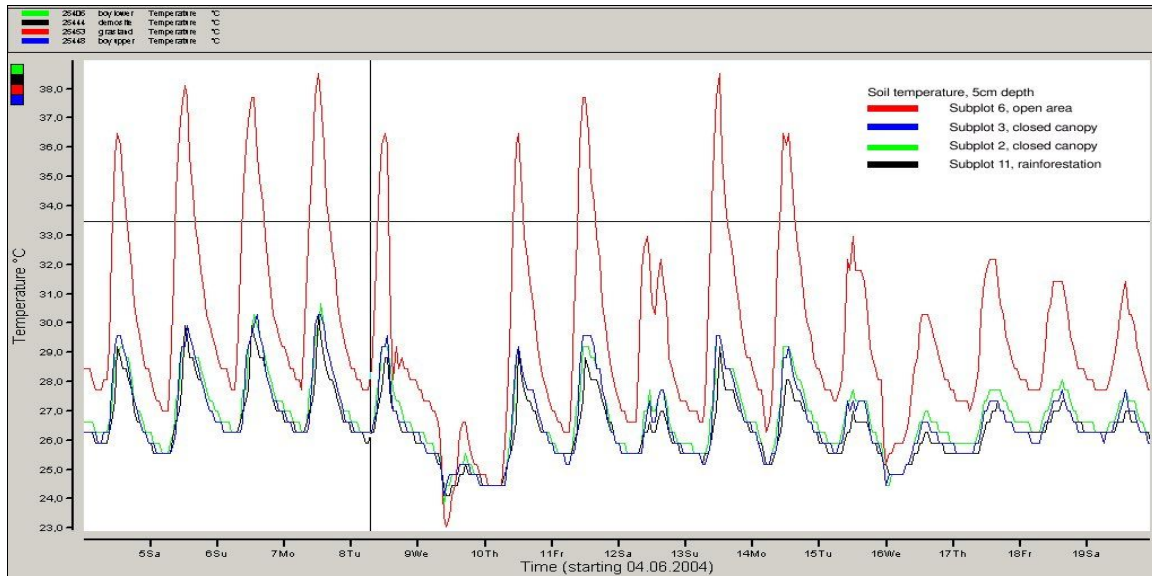
Figure 66: Soil temperature in 5cm depth under selected plots during leaf decomposition experiments (June 4th to 19th, 2004)

The experiment was designed as a comparative short-term assessment of subplots rather than sequential deinstallation to estimate the temporal course of decomposition. Decomposition rates are given as mass loss after certain periods, not as yearly k-rates, as these differ between seasons.

During an exploratory experiment with fresh *Leucosyke sp*. leaves[76] on extreme spots in Cienda (fig.67), the comparatively highest decomposition rates in subplot 6 show, that extreme temperatures did not hamper biological activity, at least as long as soil moisture was sufficient. Rainfall during the exposition period (June 4th- 20th, 2004) amounted to 202mm and was evenly distributed. Under these optimum conditions, easily decomposable substrate, high and balanced temperatures and moisture, decomposition ranged between 46 and 75% within 16 days.
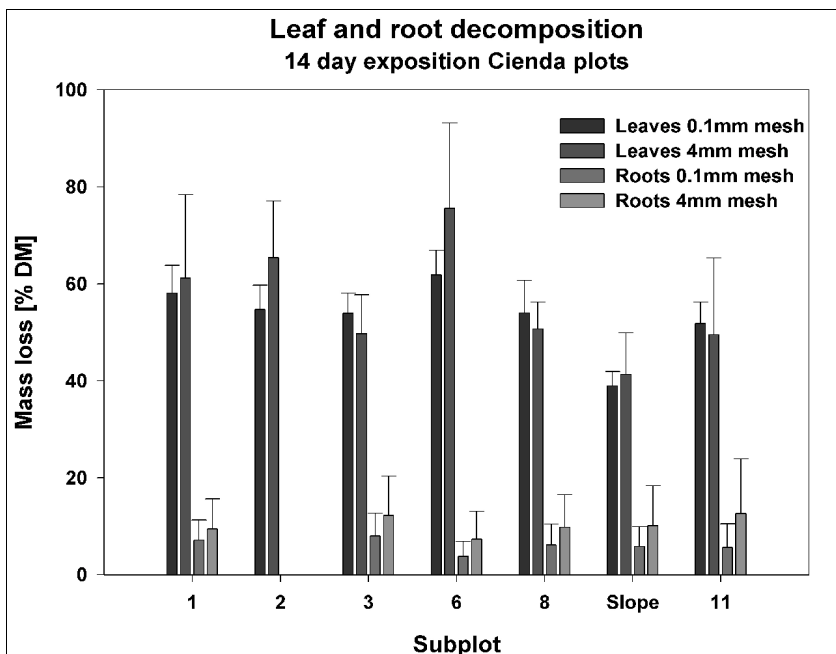
Where significant differences existed, decomposition of *Leucosyke sp*. in the 4mm mesh capsules was higher than for 0.1mm. A ranking for fine and thick mesh minicontainers gave an almost identical sequence and a correlation coefficient of 0.83. Generally, only subplot 6 differed

Figure 67: Decomposition of leaves and Cocos fine roots in Cienda 2004 (note that exposition periods were not the same)

---

76 An easily decomposable substrate

significantly from the others.

During a second experiment with *Cocos* fine roots (Aug 21st – Sep 4th), rainfall was not more than 80mm most of which fell during two events and it can be assumed, that water stress was relevant at least on the open subplot 6. Ranking differed more between mesh widths and the correlation was only 0.61. Especially for the demo site, the role of the mesofauna is evident. Subplot 6 shows by far the lowest decomposition rates for both decomposer groups. On the other hand, similarly low decomposition rates would have been expected for the slope plot, an exposed SW-slope with grass vegetation.

Another root experiment including all ten subplots of the new plantation was set up for a more detailed insight in decomposition dynamics (fig.68).
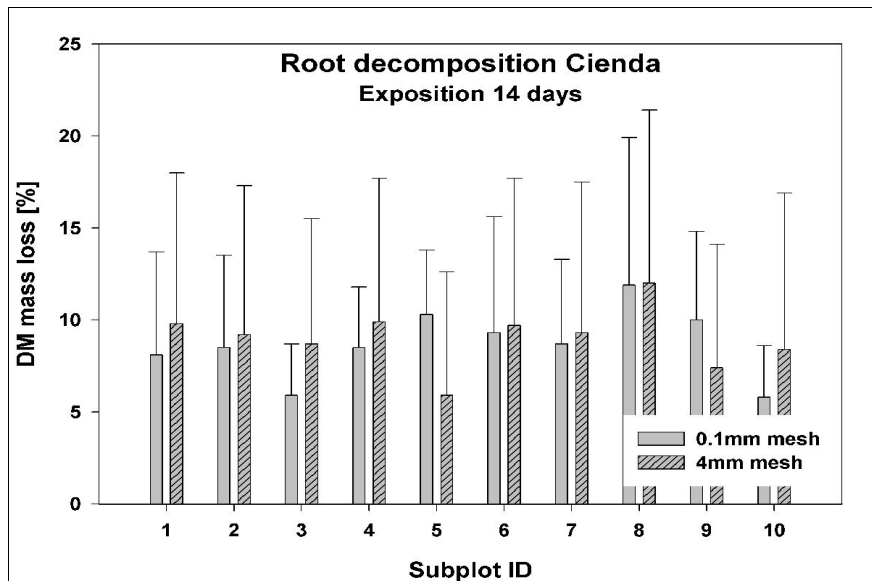

Figure 68: Decomposition of Cocos fine roots in Cienda, exposition

Decomposition of coconut fine roots was slower than expected and exposition period still too short for clear trends to develop. To cover all subplots, numbers of replicates had to be reduced at the cost of higher coefficients of variation, in average 53% for the 0.1mm mesh and 88% for 4mm mesh. The greater statistical spread for 4mm can be ascribed to higher mobility and food consumption of the mesofauna compared to microorganisms: Decomposition of 100% was found more oftenly in the 4mm capsules than in the fine mesh and young earthworms lived in some of the 4mm capsules. This and the velocity of the process indicate that decomposition of lignified material depended to a lesser extent on saprophytic fungi. Decomposition rates of adjacent subplots 1&2 as well as 6&7 were almost identical.

With respect to the relatively high root decomposition rates for 4mm mesh in the least disturbed and most forest-like demo plot, DAUB (2002) found, that certain arthropods play an important role with ongoing succession. Another explanation for the larger contribution of the mesofauna could be the higher clay contents of the demo plot topsoil, which can inhibit microbial activity (LAVELLE & SPAIN 2005) and decomposition. The same applies for pedogenic (Fe-, Al-) oxides, which form organo-mineral complexes inhibiting decomposition (VELDKAMP 1994). Both oxalate- and dithionite- extractable Al and Fe were found in higher concentrations in the demo site soil, but also in profile PN3, corresponding to subplots 6 and 7.

5.1.7 Root length and weight density

Roots can make up 20-50% of all carbon inputs in forest soils and especially in the tropics help to stabilise OM rather than easily decomposable leaf litter does (ZECH ET AL. 1997). Fine roots, generally defined as <2mm in diameter are often concentrated in the topsoil (e.g. CUENCA 1983), decisive for nutrient uptake and root litter, but do not contribute significantly to root biomass in old-growth forests (CLARK ET AL. 2001). Distribution and density of roots were interpreted in addition to data on PAR and litter production as all reflect different aspects of stand density. While litter provides the seedlings with nutrients and improves soil climate, the expected effects of PAR were protection from as well as competition for radiation, and the role of roots was mainly competitive with respect to water and nutrients, especially during the dry season in dense stands like subplot 11.
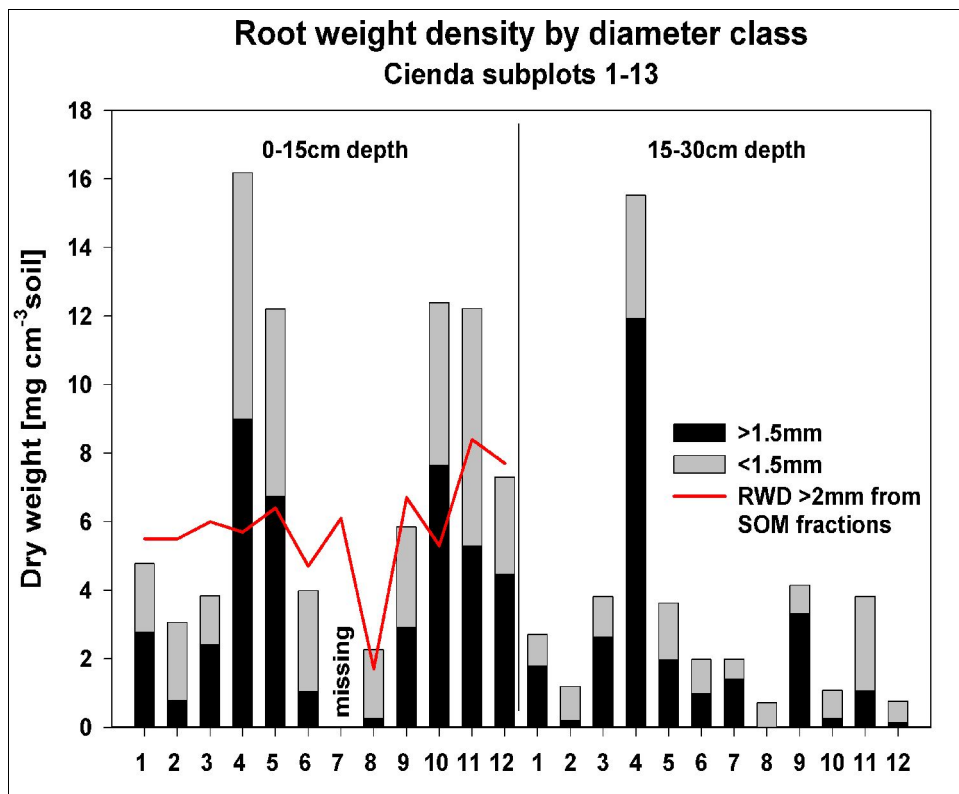

Figure 69: RWD of Cienda subplots. For the bar chart n = 1. The curve indicates composites of 12 samples per subplot as taken for OM fractions analysis. Note that for OM samples threshold diameter was 2mm and for RWD samples 1.5mm

One sample per subplot was analysed for root length density and root volume. These exploratory experiments gave a rough insight on distribution of roots in 0-15 and 15-30cm depth, ordered by root diameter classes. Correlation coefficient was 0.69 for total litter production vs. RLD 0-15cm, supporting the observation of GAISER (1993), that root growth depends on the existence and thickness of a litter layer. However, for a statistical analysis, root weight density (RWD) data, as root weight per soil volume [mg cm^{-3}], were preferred. Apart from one sample per subplot taken from 0-15 and 15-30cm and segregated into > and < 1.5mm diameter fractions, another more representative dataset was available. These were composite samples of 12 single samples per subplot each, which had been collected for SOM fractionation. Only roots from 0-15cm depth and of > 2mm diameter were included.The red curve in fig.69 stems from the SOM fractions' sample collective and

gives statistically more solid values as each sample is composed of 12 subsamples. Bars show RWD of only one sample, namely the B series of RLD and root volume (not shown). SOM-RWD values correspond to B series-RWD less than to RLD and root volume (correlation coefficients 0.44; 0.51; 0.57) in 0-15cm depth. The most 'forest-like' subplots by appearance, 1-5 and 11, are those with the highest root biomass. RWD 15-30cm shows the relatively higher proportion of the closed-canopy subplots 1-5 with respect to coarse roots and also corrects the very low values per subplot for RLD and volumes. Subplot 11 is clearly higher in RWD 15-30 than 12, an adjacent fallowed field. Subplots 6 and 7, Imperata / fern, are as low as expected in 15-30cm. RWD values are in the same range as such found for one to ten-year old cocoa and *Gliricidia sepium* systems in Sulawesi by Sᴍɪʟᴇʏ (2006). As general trends over all samples, subplots 3-5 and 11 had the highest values for all observed root parameters. Subplot 8 was by far the lowest in all categories. Subplot 9 showed surprisingly high values even for the lower depth (possibly due to loosening of the soil during planting and harvesting of cassava in 2003). As in Marcos, where Gmelina trees were parametrised, roots often extended widely in a lateral direction, especially on clayey horizons in the subsoil (see also Aᴋɪɴɴɪꜰᴇꜱɪ ᴇᴛ ᴀʟ.1999).

5.1.8 PAR measurements

Photosynthetic active radiation (PAR) is measured in W m^{-2} or µE m^{-2} s^{-1}, but expressed here as % of a reference PAR above canopy. Measurements were conducted under clear skies during midday hours. Values in open areas exceeding the reference were set 100%.
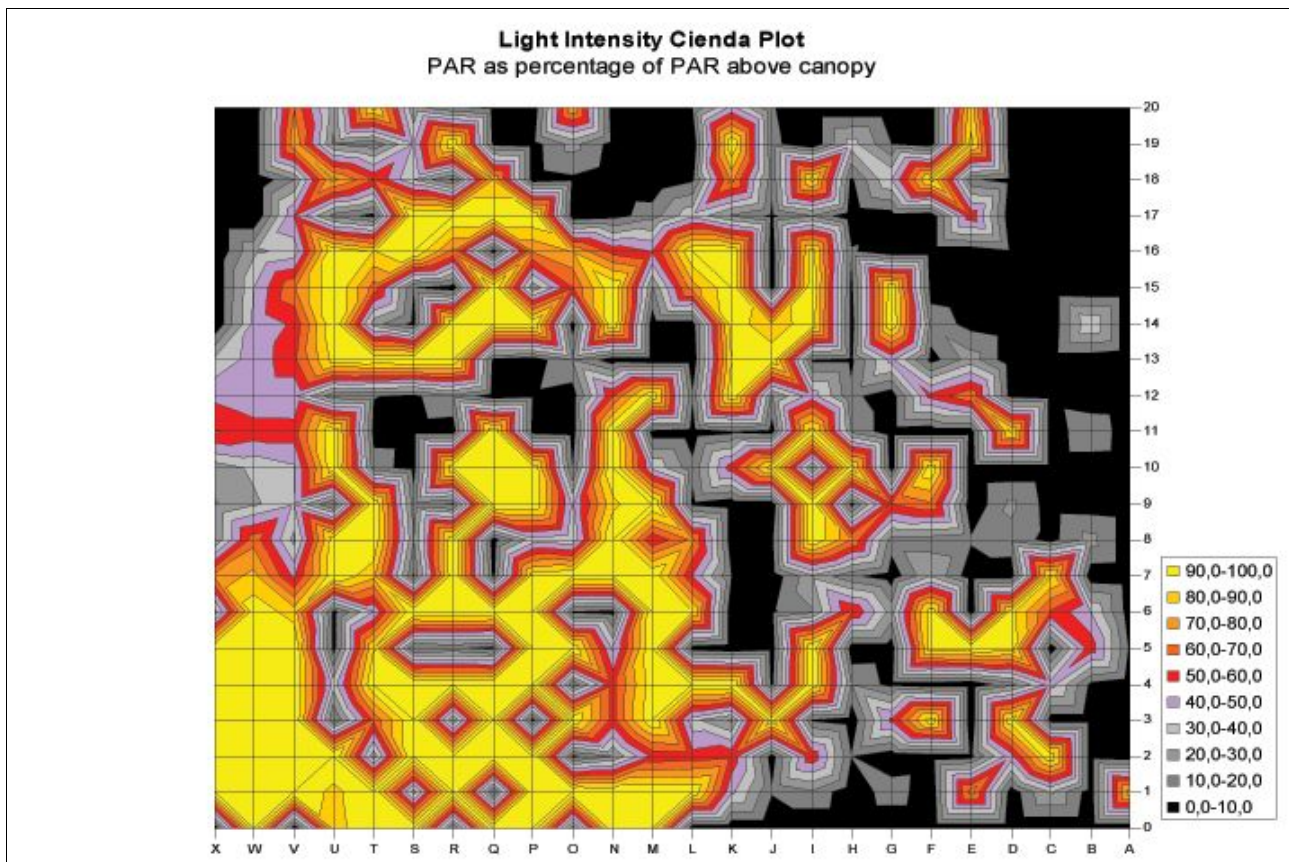

Figure 70: Photosynthetic active radiation as percentage of PAR above canopy

Fig.70 shows a map of PAR over the entire plot; note that the upper parts of lines A-D and V-X are outside the plot boundaries and were not planted. These areas appear black.

Light regime differed clearly between subplots. Numbers 1-5, under extensive management and denser canopy cover, were generally less exposed to sunlight, numbers 6, 7 and 9 most. An indirect effect of light intensity can be observed in the strip from K-J 12 upwards. The overstorey in this area was relatively open and the undergrowth covered by a thick mat of *Pueraria phaseoloides*, which strongly affected plant survival. Averages for PAR per subplot are given in table 14.

For correlations between PAR and growth parameters (see 5.1.9), values for expanded zones around the subplots were used to increase numbers of plant individuals in each plot and to cover the whole area. Plot margins and corridors between subplots were excluded from these zones. PAR values of the subplots *sensu strictu* and the expanded zones are listed in table 14, were low percentage indicates dense canopy.

Table 14: Average PAR per subplot and expanded area around the subplot

Subplot #	Mean PAR subplot [%]	Mean PAR zone [%]
1	28	37
2	18	27
3	21	27
4	38	20
5	28	23
6	69	75
7	62	60
8	39	46
9	59	63
10	56	37

In both cases, the less intensive land use under canopy can be ranked apart from the more open area under different tenure. However, subplots 8 (subplot) and 10 (expanded zone) do not differ significantly from 1-5.

5.1.9 Synopsis of environmental parameters

Principal component analysis (PCA) aggregates parameters with similar trends to components. This method was used to
- facilitate an overview of the numerous parameters and, if possible, reveal underlying influences,
- explore the variance between subplots explained by the different components,
- reduce the set of parameters for discussion and later to predict plant growth in a multiple regression (5.3.2).

The superior explanatory power of PCA to single factors has been underlined for soil microbial parameters BR, SIR and phosphatase by SVENSSON & PELL (2000). DINESH ET AL. (2004) used this approach for a similar experimental question. PCA reduces multidimensional single parameters into bundles or principal components, which explain a maximum of variance in the dataset. A coordinate system is projected in such a way, that the first axis underlies the most relevant component. In case of the applied varimax rotation, orthogonality of each following component to the previous one is required to accentuate contrasts between components.

Parameter groups forming the components are shaded in table 15. Among the various SOM fractions, the proportion of C, N and P in the light organic matter (C, N and P_{LOM}) were preselected, because they were expected to be most relevant for plant growth (GAISER 1993) and microbial communities (ALVAREZ ET AL. 1998). Single and cumulative percentage of observed variance explained by each component are included in the table. The first five among the identified components explain 89% of all observed variance.

Table 15: Principal components analysis (varimax rotation with Kaiser normalisation applied) for environmental parameters in Cienda

Component Matrix Varimax Rotation	Component					
	1	2	3	4	5	6
PAR	-0.817	-0.407	0.057	-0.204	-0.073	-0.066
Leaf litter	0.821	0.390	-0.132	0.065	0.053	-0.061
BR1	0.838	0.130	0.355	0.379	0.018	0.033
BR3	0.764	0.375	0.118	0.174	0.373	0.228
BR6	0.826	-0.100	0.291	0.092	0.242	0.304
BR12	0.909	0.064	0.189	0.255	0.146	0.077
BR18	0.669	0.147	-0.043	0.117	*0.661*	-0.028
BR24	0.693	0.053	0.228	0.266	*0.534*	-0.085
BR30	0.573	0.184	0.026	0.420	*0.587*	-0.153
P_{LOM}	0.777	0.361	0.454	0.044	-0.008	0.174
RWD 0-15cm <2mm	0.166	0.854	-0.033	0.204	0.412	-0.095
RWD 0-15cm >2mm	0.144	0.865	0.037	-0.068	0.357	0.064
RWD15-30cm <2mm	0.179	0.821	0.352	-0.005	-0.176	-0.102
RWD15-30cm >2mm	0.314	0.885	0.212	-0.073	-0.110	0.133
C_{mic}	0.425	0.112	0.787	0.159	0.390	-0.028
C_{mic} / C_{org}	0.394	0.164	0.813	0.049	0.375	-0.040
qCO_2	0.121	-0.152	-0.935	-0.120	0.006	-0.184
C_{org}Lol 0-5cm	0.273	-0.072	0.236	0.847	0.247	0.272
C_{org}Lol 7-12cm	0.454	-0.287	0.407	0.529	0.243	-0.071
C_{org}-EA mean	0.348	-0.117	0.274	0.824	0.312	0.089
C_{LOM}	0.213	0.338	0.595	0.648	0.151	0.145
Root decomp 0.1mm	-0.090	-0.103	0.116	-0.965	0.009	-0.065
N_{LOM}	0.275	0.259	0.438	0.309	0.582	0.170
Root decomp 4mm	-0.050	-0.058	-0.348	-0.155	-0.833	-0.192
Soil resp	0.182	0.015	0.120	0.251	0.099	0.908
Explained variance	**50.78**	**14.10**	**10.28**	**7.36**	**6.47**	**4.18**
Cumulative expl. var.	**50.78**	**64.88**	**75.17**	**82.53**	**89.00**	**93.18**

A first component was related to <u>soil microbial activity</u> as reflected by basal respiration, which is known to be strongly dependent on even-tempered microclimatic conditions (MARTIUS ET AL. 2004). Consequently, basal respiration is hampered by intense solar radiation (PAR, negative coefficient), which causes extreme temperatures and water regimes. On the other hand a closed canopy, as reflected by leaf litter, creates a more equilibrated temperature and water balance (see 5.1.6, fig.60, soil temperature, and 3.2.5, tensiometers) as well as substrate. Light fraction P was also part of component 1.

<u>Root weight density</u> of fine and coarse roots at different depths as a second factor was highly self-correlated and confirmed, that the method gave consistent results. Besides, it did not reveal much additional information on underlying interrelations between parameters.

A third component was determined by <u>microbial biomass</u>, alone and as quotients C_{mic}/C_{org} and $qCO_2 = BR/C_{mic}$. As an indicator of stress, qCO_2 was oriented oppositely to both other parameters. It was remarkable that microbial respiration and biomass were distinguished by the PCA procedure.

Fourth, all parameters related to soil organic carbon, including the light fraction, formed a factor reflecting <u>substrate availability</u>. Microbial decomposition (0.1mm mesh) of recalcitrant coconut roots belonged to the same group, possibly as an alternative substrate in case of lacking easily decomposable material (negative coefficient).

Component 5, like number 3, pointed to <u>substrate</u>, integrating labile N and decomposition, in this case of microbes plus mesofauna (4mm mesh). Interestingly, the long-term part of basal respiration (days 18 to 30, in *italics*), has a similar orientation as this group. This shows, that BR at the beginning and end of the 30- day experiment differed in tendencies.

The most interesting components are 1 and 4, as they reveal coherences between parameters, that had not been obvious before. The clear correlation between light-related and basal respiration parameters suggests a causal relationship and so does the correlation between BR and readily available P presented by P_{LOM}. A joint component for C_{org} as a reservoir and available P has been found in a PCA by JOERGENSEN & CASTILLO (2001) for young volcanic soils in Nicaragua. The case presented here points to P as a limiting substrate for microbial activity. Component 4 showed coherence between total C_{org} and C_{LOM}, which confirmed the results by independent analyses.

A restriction to stability of this analysis was, that plot means were used, so that the number of observations was limited. On the other hand, leaving out single parameters did not result in substantial changes of factor formation. For example, pH was not considered for PCA due to an incomplete data set covering only seven of the ten subplots; still components were the same and coefficients similar to a separate PCA including pH.

The applied varimax rotation seeks orthogonality of axes in order to make grouping factors best visible. This procedure identifies the most contrasting factors, but may confine more subtle findings as e.g. a further subdivision of component 1 (CODY & SMITH 1997). For this reason a promax rotation, which does not postulate orthogonality, was run on the same data set. However, the results were very similar in absolute numbers and identical with respect to factor grouping.

For further analysis sampling might be reduced to a minimum dataset, which would allow for conclusions about other parameters. For example, C_{LOM} can represent the C_{org} – group and BR after one day as the most frequently correlated parameter or after 24 days as a more stable measurement are sufficient to represent the entire BR time series. An observation in the crude correlation table had been, that BR correlations decreased in significance from day 1 to day 30. The most important significant correlations between selected parameters are compiled in table 16.

Table 16: Correlation coefficients between relevant environmental parameters at Cienda. Figures marked * are significant at α = 0.05, ** at α = 0.01 level (two- tailed test).

	PAR	Leaf litter	BR 1d	BR 24d	P_{LOM}	RWD fine 0-15cm	C_{mic}	C_{mic}/C_{org}	qCO_2	C_{org}Lol 0-5cm	C_{org}EA	C_{LOM}	Root decomp. 0.1mm	N_{LOM}	Soil resp.
PAR	1	-0.916**	-0.791**	-0.575	-0.830**	-0.564	-0.377	-0.348	-0.019	-0.394	-0.401	-0.482	0.303	-0.545	-0.208
Leaf litter	-0.916**	1	0.717*	0.558	0.733*	0.565	0.310	0.303	0.091	0.252	0.249	0.299	-0.214	0.347	0.023
BR 1d	-0.791**	0.717*	1	0.767**	0.877**	0.328	0.716*	0.662*	-0.302	0.643*	0.700*	0.683*	-0.409	0.564	0.321
BR 24d	-0.575	0.558	0.767**	1	0.613	0.413	0.763*	0.715*	-0.124	0.562	0.678*	0.502	-0.325	0.544	0.252
P_{LOM}	-0.830**	0.733*	0.877**	0.613	1	0.414	0.712*	0.712*	-0.435	0.376	0.394	0.635*	-0.096	0.607	0.346
RWD 0-15cm <2mm	-0.564	0.565	0.328	0.413	0.414	1	0.333	0.346	-0.109	0.242	0.235	0.490	-0.299	0.554	0.016
C_{mic}	-0.377	0.310	0.716*	0.763*	0.712*	0.333	1	0.991**	-0.707*	0.517	0.602	0.740*	-0.118	0.719*	0.241
C_{mic}/C_{org}	-0.348	0.303	0.662*	0.715*	0.712*	0.346	0.991*	1	-0.733*	0.412	0.494	0.692*	-0.016	0.685*	0.196
qCO_2	-0.019	0.091	-0.302	-0.124	-0.435	-0.109	-0.707*	-0.733*	1	-0.345	-0.298	-0.701*	0.039	-0.499	-0.246
C_{org}Lol 0-5cm	-0.394	0.252	0.643*	0.562	0.376	0.242	0.517	0.412	-0.345	1	0.966**	0.802*	-0.829**	0.616	0.542
C_{org}EA	-0.401	0.249	0.700*	0.678*	0.394	0.235	0.602	0.494	-0.298	0.966**	1	0.782	-0.778**	0.634*	0.423
C_{LOM}	-0.482	0.299	0.683*	0.502	0.635*	0.490	0.740*	0.692*	-0.701*	0.802**	0.782**	1	-0.609	0.775**	0.398
Root decomp. 0.1mm	0.303	-0.214	-0.409	-0.325	-0.096	-0.299	-0.118	-0.016	0.039	-0.829**	-0.778**	-0.609	1	-0.241	-0.304
N_{LOM}	-0.545	0.347	0.564	0.544	0.607	0.554	0.719*	0.685*	-0.499	0.616	0.634*	0.775*	-0.241	1	0.336
Soil resp.	-0.208	0.023	0.321	0.252	0.346	0.016	0.241	0.196	-0.246	0.542	0.423	0.398	-0.304	0.336	1

Due to the narrow range (5.44 – 6.01), influence of pH was less powerful than for the paired plots discussed in chapter 4. Increasing pH was related to lower SOM and C_{LOM}. As the latter are substrates for microorganisms, pH was also weakly negatively correlated to microbial activity (BR) and biomass (C_{mic}), and significantly to higher *specific* respiration (or qCO_2 = BR/C_{mic}) indicating lower metabolic efficacy. Microbial litter decomposition in fine mesh minicontainers and pH were highly correlated.
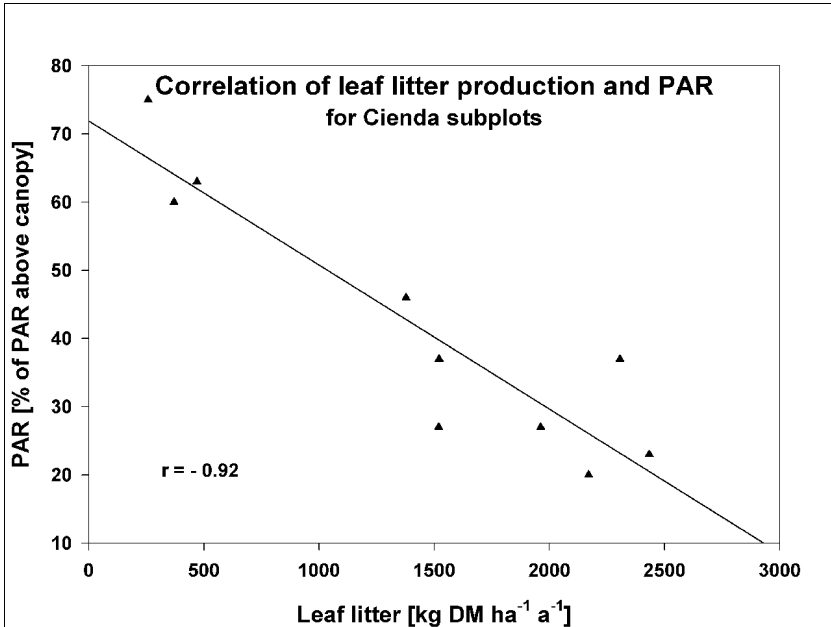
Photosynthetically active radiation (PAR) is part of and represents solar radiation which is attenuated by canopy. PAR measured in the understorey represented density of the canopy cover and was negatively correlated to root weight density and leaf litter production (fig. 71).

Intense solar radiation causes extreme surface temperatures and reduces topsoil moisture, which is crucial for microbial activity. Thus PAR can indirectly indicate stress for plants as well as microorganisms. Consequently, PAR was significantly negatively correlated to microbial respiration (fig.72). Correlations of PAR with C_{mic}, C_{org}, C_{mic}/C_{org} and C, N and P in LOM were also negative. As high PAR seems to coincide with unfavourable conditions not only for microorganisms, the respective subplots will deserve special attention in context with the growth of abaca (5.2).

Figure 71: Correlation of leaf litter production and PAR for expanded Cienda subplots. Coefficient of determination $r^2 = 0.84$

In contrast to PAR, leaf litter stands for the improvement of microclimate – conservation of soil moisture and dampening of temperature extremes – and the provision of substrate for microorganisms and plants. Positive correlations to C_{mic} have been reported by MAO ET AL. (1992), while in this study correlation with BR was more significant. In conclusion, leaf litter was a more integrated measure for canopy density than a snap-shot captured by a light sensor, but at the cost of higher fuzziness[77].
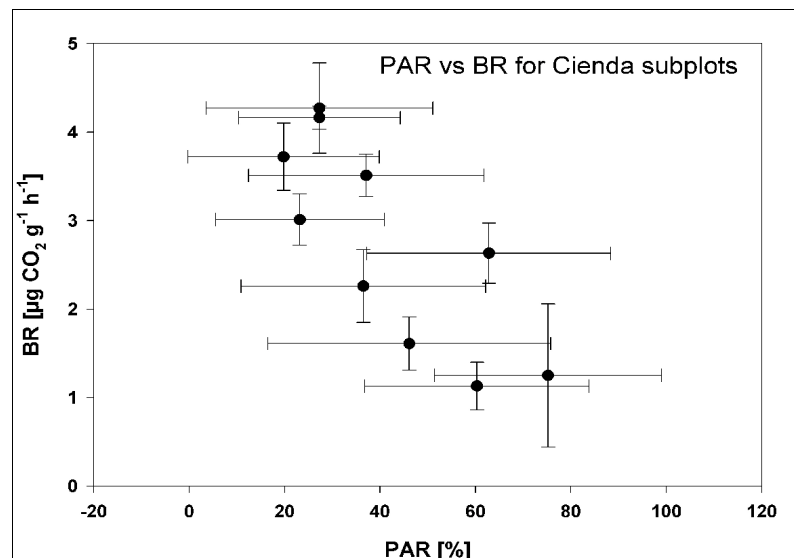

Figure 72: Correlation of PAR and BR at Cienda subplots

---

[77] especially, when different tree species are involved.

SOM as source of C_{LOM}, N_{LOM} and P_{LOM} determines the size of the microbial population (C_{mic}) and respiration as indicated by the significant positive correlations of these with C_{org}. Positive correlations between C_{mic} and BR on one hand and LOM on the other have been found by GREGORICH ET AL. (1994). The correlations presented here also agree with findings of SVENSSON & PELL (2000), that C_{mic}-SIR is controlled by availability of C *and* N, whereas BR depends more on quantity and quality of carbon, here represented by C_{LOM}.

The mutual interrelationships between PAR, leaf litter and microbial activity as well as the context between C_{org} and C_{LOM}, as explained before, are reproduced in the component clusters of the PCA, which is based on linear correlations. Relevance of the aggregated parameters for plant growth will be assessed later.

In summary, tendencies of all C-related parameters including basal respiration and C_{LOM} as well as N_{LOM} and root weight density were concordant over subplots. Reflecting present biomass, shade and management, subplot 6-8 appeared less suitable for tree planting than 1-5 and 10. Subplots could be grouped, the latter accordingly to high contents of the most important parameters C_{org}, C_{mic}, C_{LOM}, N_{LOM}, P_{LOM}, BR and leaf litter and low values for PAR and qCO_2. Unweighted ranking for each parameter and summing up scores would lead to the conclusion, that subplots 2 and 3 are best for plant growth, followed by the other subplots under canopy. Among 6-10, the latter come close to the first group and 6-8 would be least suitable to grow plants. The following section will show, in how far the measured environmental parameters were reflected by plant survival and growth.

5.2 Plant performance

Data on survival rates and growth of abaca and trees are presented in this section. Data on plant growth will be used later (chapter 6) as a reference for model calibration and validation.

5.2.1 Planted abaca

5.2.1.1 Survival rates

Abaca was included into the plot design as early-yielding component and to sequester most carbon during the first years after planting. Harvesting age is reached at 18-24 months, and continuous growth of lateral shoots (*suckers*) will lead to a relatively steady stock of biomass even after harvest of mature pseudostems at any one time.

In practice, mortality was high and growth fulfilled expectations only in few parts of the plot. An important reason for the high mortality rates was inappropriate planting material. Plants had been propagated through tissue culture and were still weak when transplanted. While plants propagated by cormus usually have enough reserves to resprout from the subterranean parts after dry spells or damage, this was not the case for the planting material used on this plot. The majority of losses (45%) occurred during the rainy season 2004/5, so that drought as direct cause of mortality can be ruled out even though two dry weeks after planting might have weakened plants. During the second year another 34% of plants died in the relatively short span between May 5th and July 4th, 2005 (fig.68 biomass), an exceptionally dry period (s. fig.8).

Another important factor influencing plant survival was maintenance by the supposed farmer cooperators. This could be observed in the upper part of lines K – N, where *Pueraria* was growing vigorously and even suffocated some trees as well as in subplots 6 and 7. In the period between July 4th, 2005, and the inventory of Feb 14th, 2006 (not shown in fig.74), the more active owner of subplots 6-10 (lines L-X) retired from the

farmers' cooperative as a consequence of the group's lacking commitment. Generally, the left half in fig.74 received more attention and care than the other side.

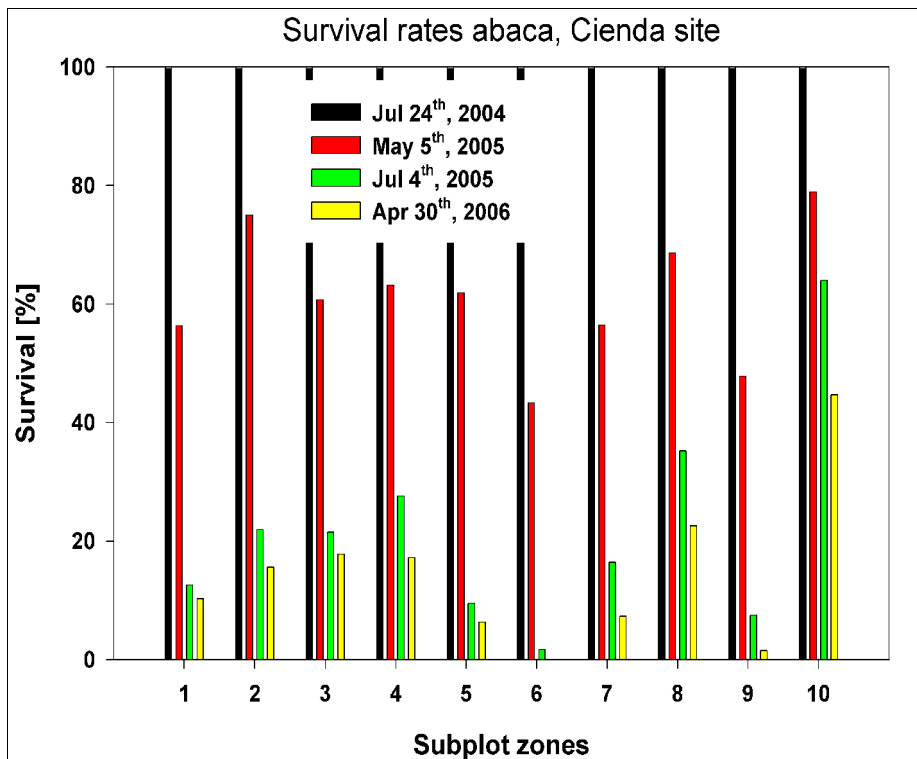Survival rates of abaca, as recorded at each subplot during inventories are displayed in fig.73.

Figure 73: Survival rates of abaca plants per subplot from July 2004 to April 2006

Overall survival rates dropped from almost 100% (first inventory July 14th, 2004) to 54.9% at May 5th, 2005, to 21.3% on July 4th of the same year and 15.3% on April 30th, 2006. Within these averages, however, variations were considerable.

5.2.1.2 Growth rates

Growth was measured as height of the pseudostem from ground level to the point of bifurcation between stalks of the youngest leaves. Height was then converted into dry matter by the use of an empiric regression. Inventories were carried out once during the first year and twice (before and after dry season) in the second and third year (see fig. 74, inventory of Feb 14th, 2006 not shown).
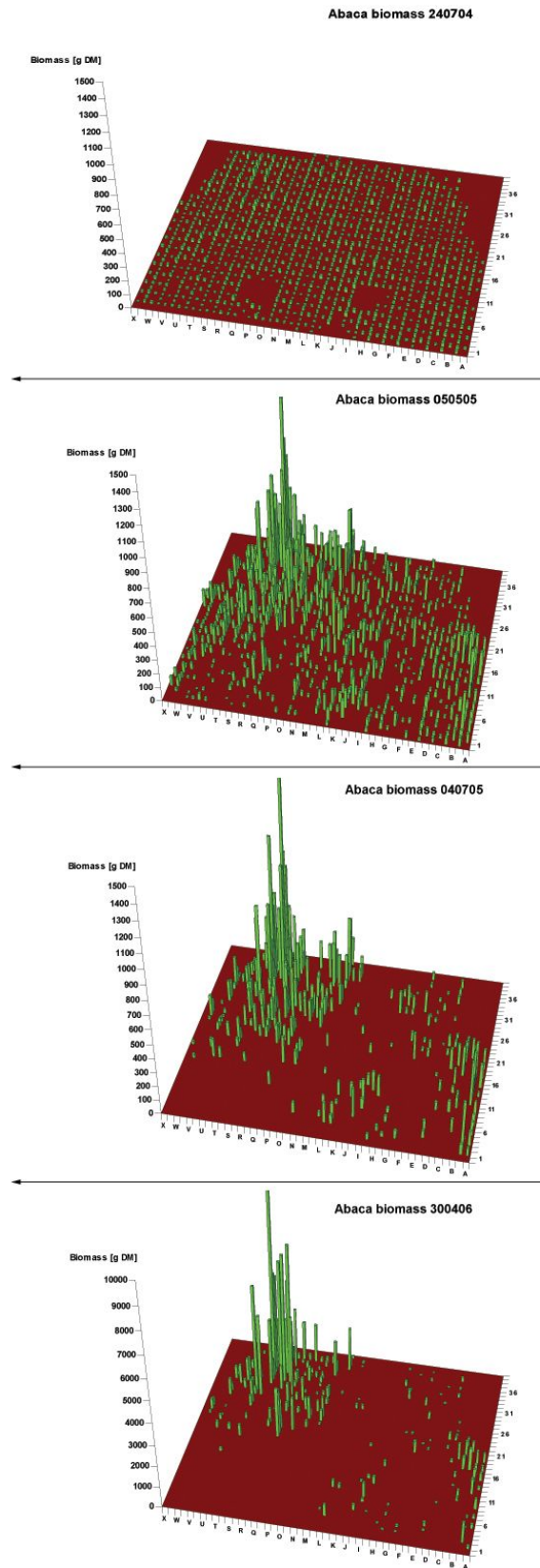
Figure 74: Growth of abaca plants at different inventory dates from 2004-6. Note different scales

The blank patches at the first inventory in fig.74 are inside subplots 1 and 6. These had not been planted as controls in order to monitor effects of abaca. The space M-X 1-8 is open area around subplots 6 and 7, in uphill direction subplots 8 (banana) and 10 (advanced fallow - secondary forest) with best overall growth rates follow. For the right half (subplots 1 to 5), growth was more uniform.

For abaca, most regressions in literature (e.g. KELLMAN 1970) are based on diameter as sole predictor for biomass, whereas for the small plants in Cienda height was more meaningful to be measured. HAIRIAH ET AL. (2001) give a diameter-height and diameter-weight regression for banana, but referring to diameters between 7 and 27cm and measured at 135cm height[78]. Moreover, plantlets bred from tissue culture showed a different habitus during their early development stages compared to abaca or banana grown from corms.

Abaca aboveground biomass at Cienda was calculated from destructive measurements of height and dry weight (n=3 over the entire range of sizes) as

$$B = 0.0772\ H^{1.828},$$

where B is biomass dry matter measured in [g] and H height in [cm]. Coefficient of determination for the empiric equation was $r^2 = 0.974$.

Abaca biomass at the consecutive inventories is shown in fig.75 as means of initially planted individuals, with dead plants considered as biomass zero[79].
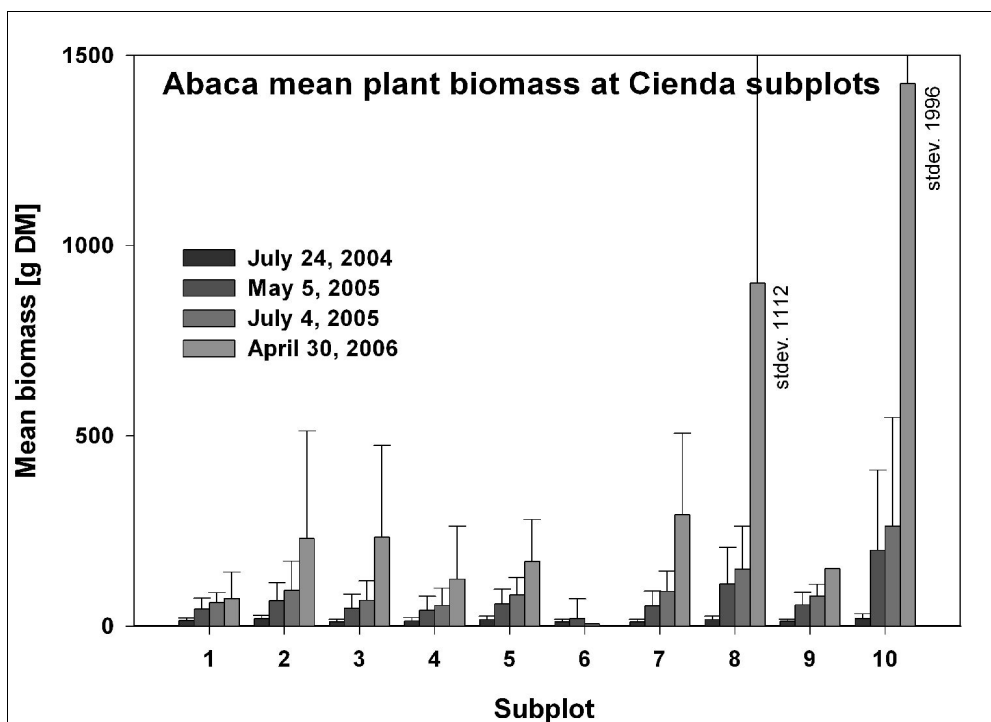

Figure 75: Mean abaca biomass per subplot at different inventory dates

---

78 Height [m] = $0.7071x^{0.6835}$, where x = stem diameter [cm] at 135cm height ($r^2 = 0.8143$).
Biomass [kg] = $0.0303x^{2.1345}$, where x = stem diameter [cm] at 135cm height ($r^2 = 0.9887$).
79 Means of living plants would have distorted the overall image and comparison of total biomass was not appropriate because of different n.

Applying a Mann-Whitney test to detect significant differences between mean plant biomass per subplot, these were generally more different at the first inventory (approx. 3 months after planting) and then became more uniform towards the second inventory. Exceptions were subplots 8 and 10, where plants started soon to grow comparably better. From inventory 2 to 3, mainly subplot 6 began to contrast more strongly as plants grew slower than in other subplots and finally died. Generally, abaca on subplots 10 and 8 developed best, followed by 7, 2 and 3. For the open area around subplot 6, no live plant remained at the last inventory. Growth was more uniform on subplots 1 to 5, under canopy.

Table 17: Differences in abaca biomass between Cienda subplots at the last inventory, April 30th, 2006. Combinations marked with one asterisk are significantly different at α = 0.05, with two asterisks at α = 0.01 level (Mann-Whitney test).

P	S1	S2	S3	S4	S5	S6	S7	S8	S9
S2	0.374								
S3	0.103	0.764							
S4	0.167	0.905	0.777						
S5	0.438	0.152	0.036*	0.057					
S6	0.010*	0.002**	0.001**	0.001**	0.046*				
S7	0.618	0.237	0.081	0.119	0.814	0.033*			
S8	0.006**	0.260	0.158	0.124	0.003**	0.000**	0.009**		
S9	0.029*	0.006**	0.001**	0.002**	0.148	0.340	0.107	0.000**	
S10	0.000**	0.001**	0.000**	0.000**	0.000**	0.000**	0.000**	0.000**	0.000**

The large differences between subplot 8 and the following subplots (see tab.17) were not always statistically significant due to the high standard deviations.

5.2.2 Planted trees

5.2.2.1 Survival rates

Survival rates were for all tree species higher than for *Musa textilis* (fig.76). As documented by Quimio et al. (1998) for the Cienda rainforestation site, even some dipterocarp trees are able to grow well under full sunlight.

Percentage survival rates per species at the last inventory are given in the legend of fig. 76. Durian and white lauan were severely affected by the dry summer 2005 (period between the inventories of April and June). In addition breakage during coconut harvest and cutting through the owners were further major causes for mortality. Pests affected mainly kalantas and rambutan (inventory data not shown) and abaca (periodic
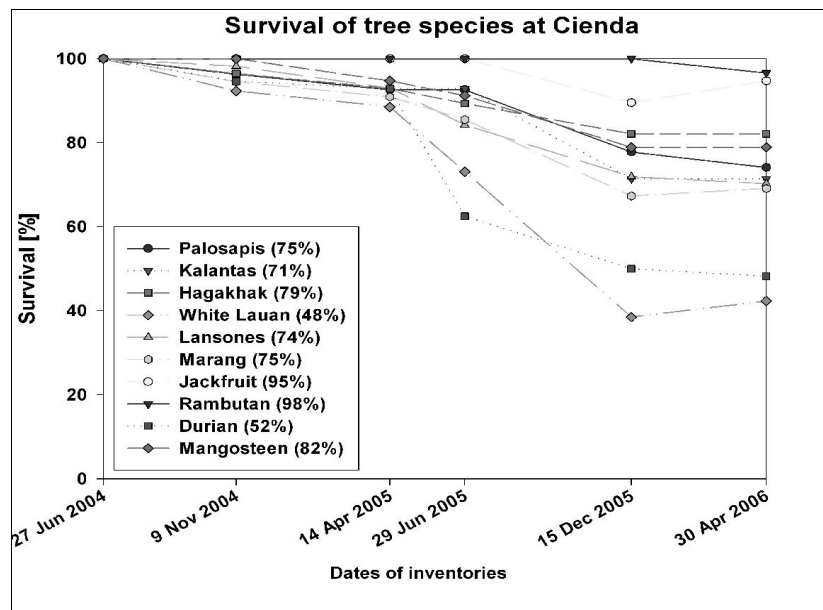

Figure 76: Survival rates for ten planted tree species from 2004-2006. Survival rates at last inventory in brackets

appearance of leaf hoppers). Intercostal chlorosis was observed for most lansones.

As for abaca, survival depended to a large extent on planting material. Especially white lauan seedlings had been uprooted just before planting and many plants dried soon. Marang wildlings were also weak, but planted later than other species, so that they were not affected by drought during the first year. Damage and mortality of durian were mainly due to breakage and cutting; another important reason was leaf-shedding as a consequence of the dry summer 2005. Some mangosteen were initially struck by the abrupt transfer from a shade-bed into open areas, but recovered soon under artificial shade of palm fronds. Among the planted timber species *S. palosapis* was the most pioneer-like, least susceptible to drought and performing best in open areas.
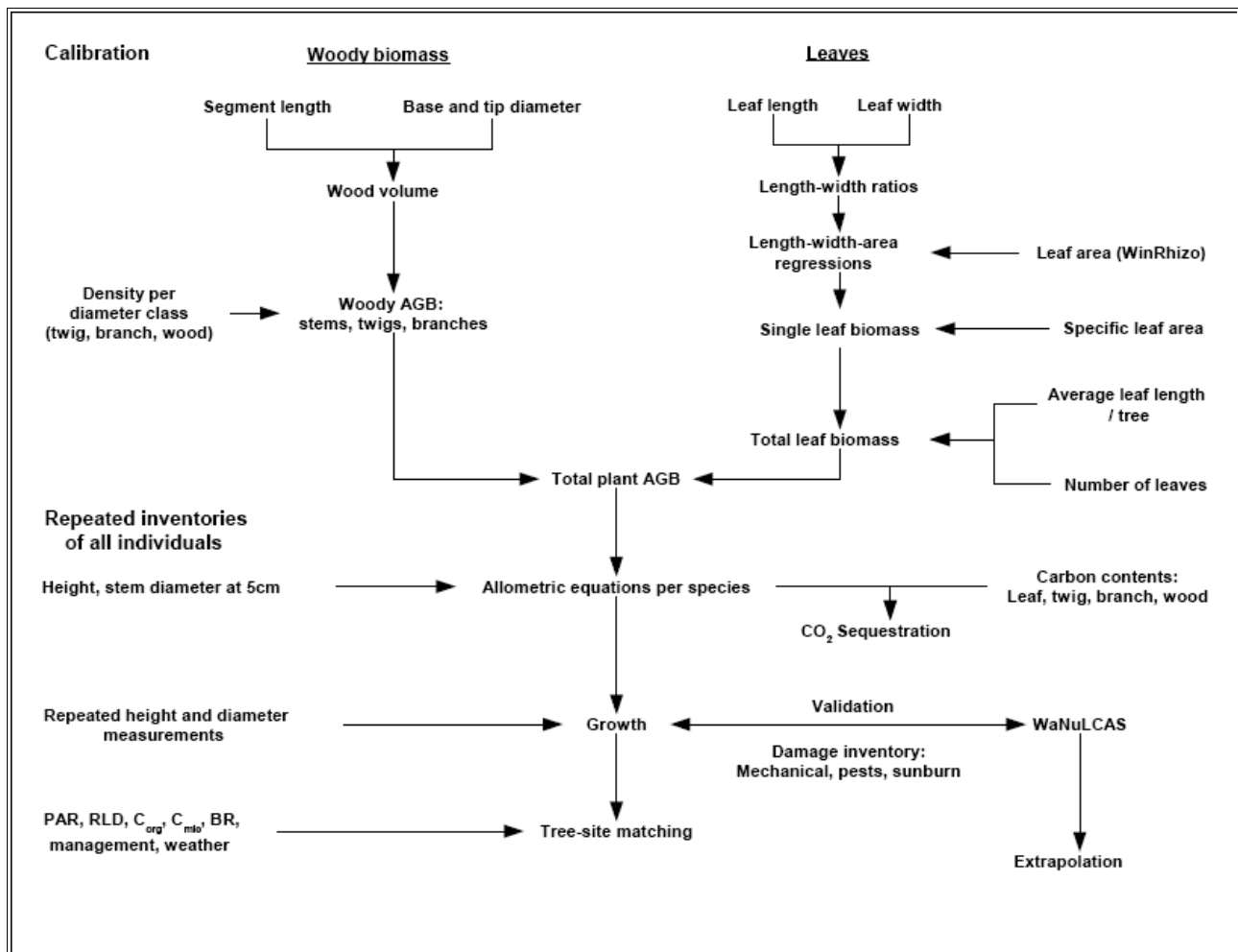
5.2.2.2 Tree growth

Figure 77: Flow chart for tree biomass measurements. All biomass data refer to dry matter.

Inventory dates and methods as well as classical biomass measurements to obtain allometric equations have been described in 2.6.4.2 -3, an overview is given in fig.77. This classical determination of plant biomass was used later to calibrate and validate WaNuLCAS data, which are based on habitus, branching pattern (FBA), C, N, P contents, specific leaf area (SLA), leaf weight ratio (LWR), lignin and polyphenolics, among others.

Wood density was mostly determined experimentally, but taken from literature where wood samples were not available. Carbon contents were determined by Walkley-Black method for leaves, twigs, branches, stems and roots of every planted species, *Cocos sp.* and undergrowth. Specific densities and carbon contents are listed in Annex 5.2.2.2.

Leaf length and width were determined for 15 to 20 leaves of different sizes per species and average length-width ratios calculated. For 3 to 10 leaves per species, leaf area was analysed using a scan or xerox and image analysis software. A combined factor of length x width proved as best predictor for leaf area. Linear or quadratic equations were of the form

$$A = y_0 + b\ l\ w \qquad\qquad \text{or} \qquad\qquad A = y_0 + b_1\ l\ w + b_2\ (l\ w)^2$$

where A is leaf area, l is leaf length and w stands for leaf width.

Equations passing through the origin were preferred, as they better reflect morphology over the entire range of leaf sizes (for equations see Annex). Coefficients of determination were 0.99 to one.

Total woody and leaf biomass were summed up for each species and allometric equations deducted.

A first approach was an empiric formula used for forests of the Humid Tropics independently of site and tree species ($B = 0.118D^{2.53}$; BROWN 1997)[80]. This was compared to an approach by v. NOORDWIJK ET AL. (2002), using a site-specific exponent c. Biomass is calculated as

$B = 0.11\rho DBH^{2+c}$ where ρ is wood density and 0.11 an empiric constant and c is derived from

$H = a\ D^c$ which describes the proportions (height to diameter) of a tree.

A generic exponent (c = 0.62) was used as suggested by the authors and in addition species-specific c-factors and their site-specific average (c = 0.934) were tested as modifications. These were compared to the values obtained by own non-destructive measurements as presented above. In modification to the proposed method, diameters at 5cm height replaced DBH as numerous trees were still smaller than 135cm.

All models overestimated measured values for AGB (see fig.78). Using the default value c = 0.62 reduced this error (species-specific c ranged from 0.64 to 1.12), and also followed the trend of measured values best[81].

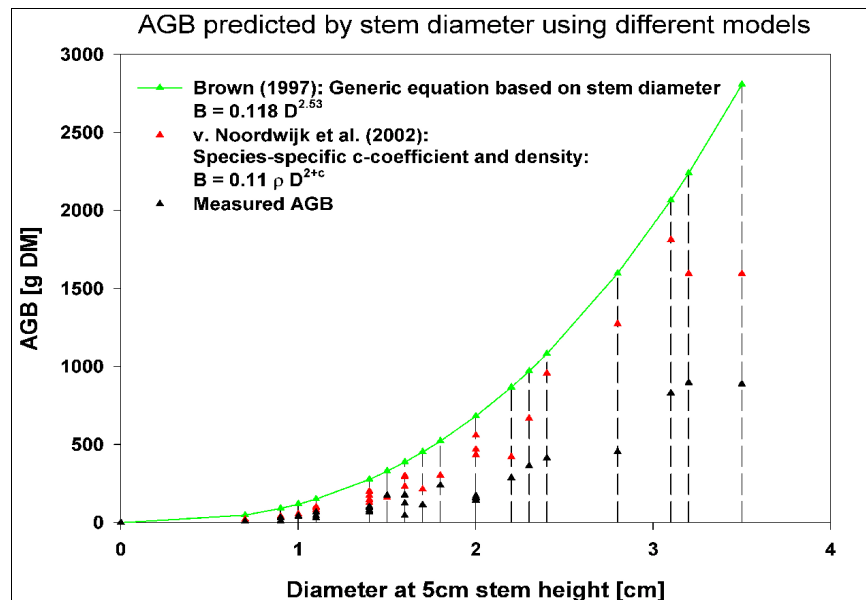As a third approach, an empiric equation based on

Figure 78: Measured AGB as compared to a generic and a species-specific model predicting AGB from stem diameter

---

80 Empiric regressions derived by foresters oftenly refer to merchantable height or volumes, not to overall biomass (WEIDELT & BANAAG 1982).

81 Note that different species are plotted in fig.75, so that equal diameters can result in different biomass.

the abovementioned geometric concept of squared diameter by height ($0.11\rho hD^2$) as suggested by KETTERINGS ET AL. (2001) was adapted to the measured values. This empiric formula was

$B = a\ (0.11\rho\ h\ D^2)^b$, as shown in fig.79.

As the predictor is a mixed factor of most influencing components, the exponent is almost 1 and the curve close to linearity. On the other hand, constant variation was not met due to height, so that diameter as predictor was preferred. Alternatively, empiric regressions were formulated for each species as shown in tab.18. For these, high
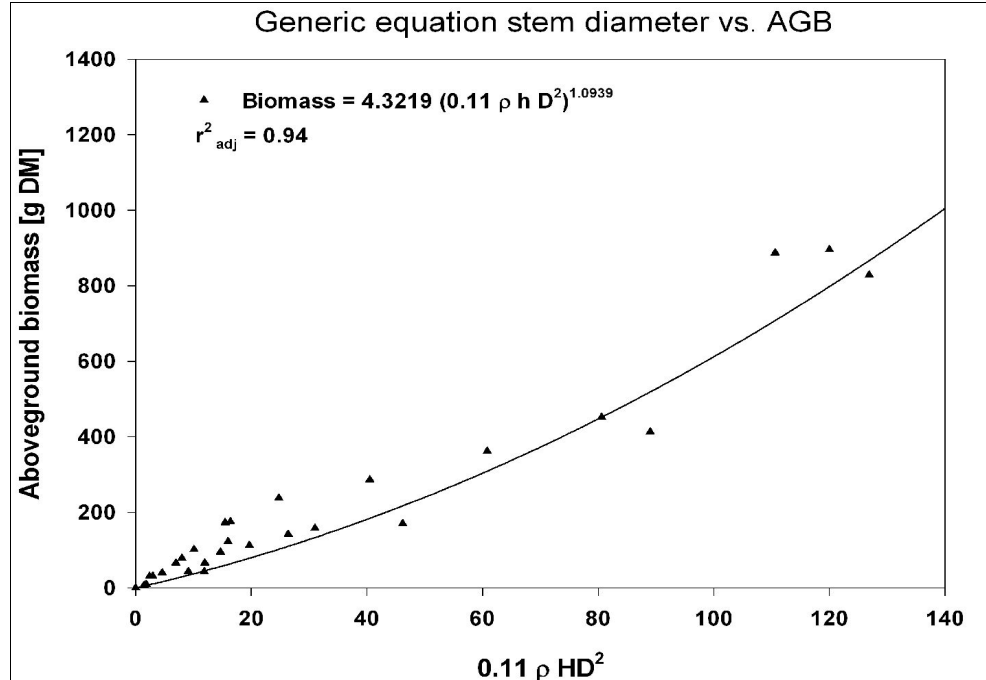

Figure 79: Empiric allometric equation based on height and diameter after KETTERINGS ET AL. 2001

coefficients of determination are due to the low number of sampled trees. Still, a generic equation for all ten species gave a similarly high r^2.

Table 18: Species-specific allometric equations for planted trees. B = biomass [g DM], D = diameter [cm].

Species	Allometric equation	Adjusted r^2
Dipterocarpus validus	$B = 19.0824\ D^{3.0651}$	0.98
Shorea contorta	$B = 36.5806\ D^{2.7693}$	0.99
Shorea palosapis	$B = 2.6216\ D^{5.9158}$	0.99
Toona calantas	$B = 67.2904\ D^{2.0594}$	0.99
Nephelium lappaceum	$B = 0.0019\ D^{13.4364}$	0.99
Durio zibethinus	$B = 18.9759\ D^{3.4375}$	0.99
Garcinia mangostana	$B = 22.8971\ D^{4.3455}$	0.99
Lansium domesticum	$B = 34.9073\ D^{2.2848}$	1
Artocarpus heterophyllus	$B = 48.4267D^{2.5907}$	0.99
Artocarpus odoratissimus	$B = 32.6774\ D^{2.8576}$	0.99
Generic all species	$B = 34.9456\ D^{2.6742}$	0.95

V. NOORDWIJK ET AL. (2002) emphasise the advantage of species-specific over generic

regressions traditionally used in forestry. As few individuals of known species were tested in Cienda, this could easily be realised, but the generic regression presented in fig.80 rendered a surprisingly high coefficient of determination and had the advantage of higher *n* relevant for statistical accuracy.

In the case of rambutan, diameters at stem base did not cover a sufficient range to produce a reasonable calibration curve (exponent >13). For this reason the empiric generic equation of all 10 species was chosen to represent rambutan growth.

For allometric equations, the general form $B = aD^b$ makes sense biologically as it leads through the origin, contrary to some linear equations which gave better coefficients of determination. The exponential regre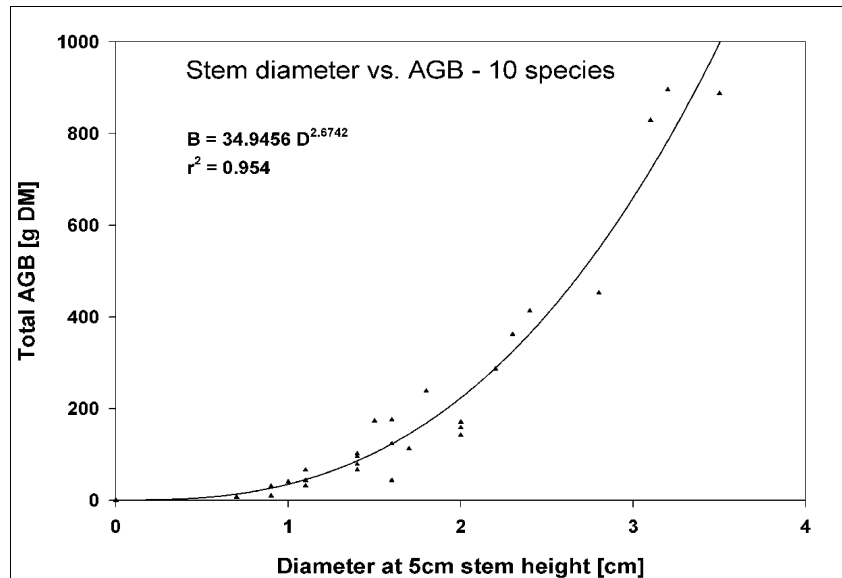ssion type has been suggested by various authors. SMITH & BRAND (1983) compiled regressions for 98 shrubs and small trees including a formula to transform dbh to diameters measured at 15cm height. Their equations covered similar magnitudes as the ones used for Cienda, with *a* values of 4-80 and exponents between 1.4 and 2.5, exceptionally 3.5. Low exponents would be important for extrapolations into the low and high range, as otherwise biomass of small plants would be under- and of tall plants overestimated. For Cienda this was not relevant, as the smallest and tallest individuals had been used for calibration.

Figure 80: Measured and predicted biomass for a generic equation based on diameter of all ten planted tree species
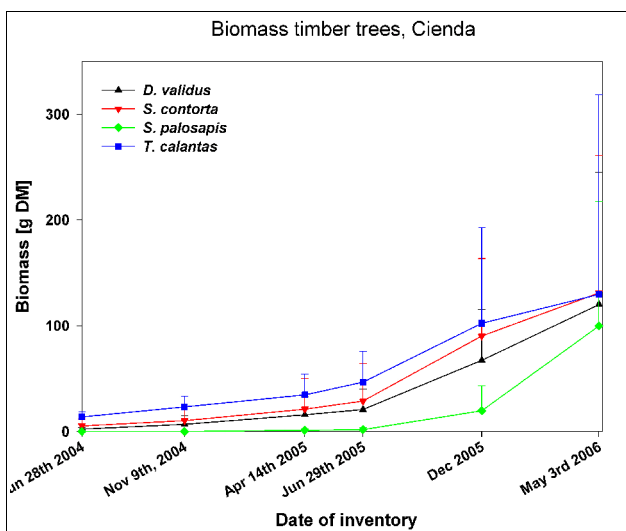
Biomass timber trees
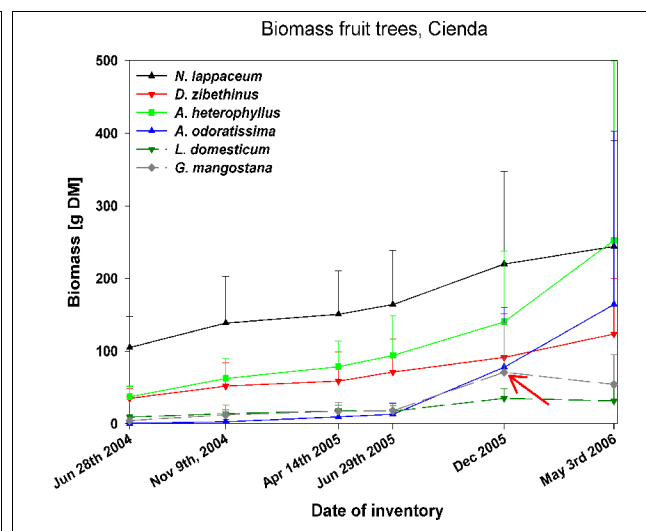
Biomass fruit trees

Figure 81: Mean tree biomass based on empiric species-specific equations.

Growth of the different species between inventories is shown in fig.81. These values are based on the empiric equations of the form $B = aD^b$ as mentioned before (tab. 18). Mangosteen and lansones are known to be slow-growing trees, while the two Artocarpus-species are fast-growing. *A. odoratissimus* was planted as uprooted wildlings and trees were smallest at the beginning, but caught up with all timber species. For mangosteen, some small trees beneath a mat of weeds were overlooked during the inventory in Dec 2005, so that the average for this date was overestimated (see arrow in fig.81, right side). Deviations from means are large, because growth is influenced by a number of interacting factors. These data have been adjusted in so far, as biomass was calculated on the basis of diameter, not height, so that mechanical breakage of tips is not accounted for.

5.3 Environmental conditions for abaca growth

Given the environmental data presented before, it was of interest to relate these to survival and growth of plants. It was assumed, that factors influencing both might not be the same or of unequal importance. Abaca was selected to evaluate growth conditions, because it contained the highest number of individuals and because differences between subplots were most pronounced.

5.3.1 Survival rates of abaca

In order to estimate the impact of factors for survival / mortality of abaca plants, logistic regressions were formulated to predict the probability of survival as depending on environmental parameters. A logit transformation is used to topple results of the predictor equation into categorical values, either 0 (here: dead) or 1 (here: survival). Thus, the odds of a chosen reference event (here: survival) can be predicted at a certain probability level (CODY & SMITH 1997).

Regressions were produced for the abaca inventories on May 5th and July 4th, 2005. These were the dates with the most balanced numbers of events and non-events. In a first ranking, the most significant single factors for the predictor equation were identified and then integrated into the logistic model as long as they were significant[82], contributed to better fit of the model, and increased either concordance or sensitivity / specificity of the model.

The selected logistic model for May 5th, 2005, contained the independent parameters C_{mic} / C_{org}, BR, $C_{org\ 0-5cm}$, leaf litter production, slope position and decomposition. Leaf litter production as an integrated descriptor of light, soil temperature and moisture was given preference over PAR as a predictor for mortality, because the latter reduced model fit below acceptable thresholds. The parameter slope is a positive equidistant index starting with 0 from the footslope. It was entered because of its numeric, not causal explanatory power, as it represents an aggregated item of not well-defined components. Erosion processes, as shown in chapter 3, may influence this factor. Other implicit factors are management and land use history, which differed in the lower and upper part of subplots 6-10. Coefficients and p-values of the variables are presented in tab.19. Negative coefficients indicate negative influence of the respective parameter on the odds of the reference event *survival* to occur; this is also expressed by odds ratios < 1. All factors were significant at the 95% level (see Pr > χ^2).

---

82 If variables are intercorrelated, they will influence each others' significance when entered into the regression.

Table 19: Selected parameters for logistic regression with their coefficients and p-values. Dependent variable was survival on May 5th, 2005.

Parameter	Coefficient	Odds ratio	Pr > χ^2
Intercept	-23.1622		0.0018
C_{org} 0-5cm	3.9790	53.462	0.0012
Decomposition roots 0.1mm	0.5213	1.684	0.0026
Leaf litter production	0.0260	1.026	0.0009
Slope	0.0203	1.020	0.0121
C_{mic} / C_{org}	-0.7766	0.460	0.0014
BR 6d	-1.1798	0.307	0.0089

Pearson (P = 0.5098) and deviance (P = 0.2025) tests for goodness of fit showed that the model predicted the dependent data well. Concordance of expected and predicted events was 61.1% (at 1.6% ties), meaning that in three out of five cases events occurred as predicted. The equation to predict odds of survival reads as follows:

Log (odds) = -23.1622 + 3.9790C_{org} [%] + 0.5213decomp. [%] + 0.026 leaf litter [kg ha^{-1}a^{-1}] + 0.0203 slope [ ] - 0.07766C_{mic}/C_{org} [%] - 1.1798BR [µg CO_2 g^{-1} h^{-1}].

Table 20 shows the number of events and non-events and their proportion, their correct or non-correct prediction and the deducted sensitivity and specificity of the model at selected probability levels. Sensitivity or *true positive rate* characterises the proportion of correctly predicted reference events, specificity or the *true negative rate* the share of correctly predicted non-events. To predict the non-event 'mortality' on the basis of the given parameters, a high specificity would be required; this would be met at a probability level of 0.82, but at the cost of no sensitivity. To make a statement of balanced specificity and sensitivity, a cut-off at 0.620 could be chosen, at 59.2 and 53%, respectively.

Table 20: Classification table for the logistic regression of inventory 050505.

	Correct		Incorrect		Correct	Sensiti-vity	Specifi-city	False positive	False negative
Probability level	Event	Non-event	Event	Non-event	%				
0.440	519	0	313	0	62.4	100.0	0.0	37.6	.
0.500	464	59	254	55	62.9	89.4	18.8	35.4	48.2
0.600	331	149	164	188	57.7	63.8	47.6	33.1	55.8
0.620	307	166	147	212	56.9	59.2	53.0	32.4	56.1
0.700	90	289	24	429	45.6	17.3	92.3	21.1	59.7
0.800	46	298	15	473	41.3	8.9	95.2	24.6	61.3
0.820	0	313	0	519	37.6	0.0	100.0	.	62.4

Among all tested logistic regressions for the inventory of July 4th, 2005, the same selected variables (see table 21) as included for May 5th rendered the best combination for goodness of fit, significance, concordance and sensitivity / specificity.

Table 21: Selected parameters for logistic regression with their coefficients and p-values, ordered by odds ratios. Dependent variable was survival July 4th, 2005.

Parameter	Coefficient	Odds ratio	Pr > χ^2
Intercept	-23.3842		0.0103
C_{org} 0-5cm	3.9578	52.341	0.0072
Decomposition roots 0.1mm	0.4504	1.569	0.0395
Slope	0.0510	1.052	<.0001
Leaf litter production	0.0341	1.035	0.0027
C_{mic} / C_{org}	-1.3541	0.258	<.0001
BR 6d	-1.6191	0.198	0.0021

Coefficients of all variables were of the same algebraic sign and, if compared to each other, of similar magnitudes for both inventories. Between inventories, however, odds ratios for BR and C_{mic}/C_{org} decreased to 64 and 56% of their respective values at the May inventory, giving them even stronger negative impact on the event survival to occur.

Concordance reached 74.8% (at 1.5% ties), but at clearly lower probability levels, with a balanced cut-off for sensitivity and specificity at 0.260 (table 22).

Table 22: Classification table for the logistic regression of inventory 040705.

	Correct		Incorrect		Correct	Sensiti-vity	Specifi-city	False positive	False negative
Probability level	Event	Non-event	Event	Non-event	%				
0.040	214	0	618	0	25.7	100.0	0.0	74.3	-
0.100	203	122	496	11	39.1	94.9	19.7	71.0	8.3
0.200	158	365	253	56	62.9	73.8	59.1	61.6	13.3
0.260	146	426	192	68	68.8	68.2	68.9	56.8	13.8
0.300	126	469	149	88	71.5	58.9	75.9	54.2	15.8
0.400	73	577	41	141	78.1	34.1	93.4	36.0	19.6
0.500	73	577	41	141	78.1	34.1	93.4	36.0	19.6
0.600	73	577	41	141	78.1	34.1	93.4	36.0	19.6
0.700	0	618	0	214	74.3	0.0	100.0	-	25.7

When a full logistic model, including all parameters, was formed, results would hardly improve compared to the reduced models above. This was mainly due to the exclusion of variables which were linear combinations of other variables. Most additional parameters were of low significance. PAR as such did not contribute significantly to the explanation of survival / mortality rates (P > 0.75). On the other hand leaf litter and BR, which were highly correlated to PAR, did. This is remarkable, as PAR values were available in high density and leaf litter data as subplot means. Yet, considering that the effect of light on plants follows an optimum curve, it is difficult to encounter any linear or logistic relationship between PAR and survival.

From a common sense perspective it appeared obvious from an early stage, that drought was the main causal factor for mortality of abaca plants. The species has been described as typical for successional stages after selective logging (KELLMAN 1970) like banana in secondary forests (MILZ 2001), which implies protection through a closed canopy. ECKSTEIN & ROBINSON (1996) found, that water stress during few consecutive days can result in

massive reductions of photosynthesis in banana[83]. As mentioned before, mortality was high within a short period of time, indicating that it was rather caused by stressors than lack of nutrients. Consequently, available N and P from the LOM fraction did not play any role for survival in the regressions. Large leaf area and low mutual shading of leaves make Musaceae susceptible to transpiration stress and temperatures of 38 – 40°C can halt leaf growth (RODRIGO ET AL. 1997). Although drought delimits nutrient availability and uptake, dehydration due to high transpiration would be the more probable reason for mortality. Another indicator pointing to influence of water was the importance of C_{org}. Soil organic matter serves as a reservoir for soil water and interrupts capillary rise from the subsoil. If the nutrient aspect had been the crucial component of SOM, then C_{LOM}, N_{LOM} and P_{LOM} would have been of major importance, which was not the case.

One factor that changed clearly during the experiment was management of the plots. While this consisted of uniform weeding after installation and declined to zero towards the second year, the owner of subplots 6 - 10 started then to engage more on the upper part of his field, subplots 8 and 10. In a single-factor logistic model based on management as a categorical variable, concordance rose from 0 to 29, then 46 and remained at 44% for the subsequent inventory dates. This indicates, that management played an increasing role for survival from the second year on. The relevance of planting material and management could be observed at a comparable abaca field planted under full sun, but from corms, and being weeded continuously. The plantation showed survival rates of nearly 100% and uniform growth, comparable to some of the best plants at subplot ten in Cienda. The plantation had been installed in August 2004 at LSU (the plot has been described in chapter 4 as LSU annuals paired plot) and showed C_{org} levels below most Cienda subplots. With respect to the planting material, it was supposedly the small size of the plants rather then tissue culture techniques *per se*, which led to high susceptibility to drought stress. ECKSTEIN & ROBINSON (1996) remarked that tissue culture was becoming more popular in the 1990s, because banana plants produce up to 60% more root DM and 100% more leaf area during the first five months compared to suckers. Under water stress a stronger increase in leaf area than root biomass may be fatal. As a rule of thumb for South African banana growers, ECKSTEIN & ROBINSON recommended, that soil water potential should not drop below -15 to -20kPa for young plants from tissue culture. This corresponds to pF 2.3. As shown under 3.2.5, potentials as low as 2.8 or -60kPa were reached at subplot 6 during dry spells.

PAR artificially reduced to 31% of open area values led to a decrease in photosynthesis of banana to 73%, but transpiration decreased even more sharply to 62% (ECKSTEIN, ROBINSON & FRASER 1997). Total cropping cycle (planting – harvest) was elongated by 11 weeks and the time span from planting to flower, corresponding to harvest for abaca, by almost 6 of 53.3 weeks.

5.3.2 Abaca growth

Multiple regression procedures were used to predict abaca growth from the parameters presented before. As dependent variables, two types of plant data were used: Biomass calculated from heights at each inventory and growth as difference between two inventories. This was done to reduce covariance caused by potentially unequal initial biomass at planting.

On the basis of subplot means, linear regressions were formed. In a first approach, a reduced set of independent variables was selected using a maximum r^2 procedure. Among the best predictors, the backward elimination procedure was applied. Strongly

---

[83] Under South African conditions, 12 days of water stress caused photosynthesis to drop by 79%.

correlated or similar parameters were reduced to as few representative variables as possible in order to avoid overfitting. For the same reasoning, it was aimed at employing PCA components integrating various single parameters. In addition C, N and P_{LOM} as percentages (C, N and $P_{LOM\%}$) in the entire sample were replaced by absolute concentrations in [mg kg^{-1}] after some preliminary tests; these parameters are denominated C, N and P_{LOMabs}. Equations listed in table 23 with their respective coefficients of determination and P-values were selected to best predict biomass and growth.

Table 23: Multiple regressions for prediction of abaca aboveground biomass and growth.

Dependent variable	Equation	r^2	P
Biomass July 24th, 2004	$y = -112 + 0.13P_{SOM} + 486.4N_{LOMabs} -0.21qCO_2 -15.7BR30 + 20.81 C_{org\ 7-12}$	0.9665	0.0047
Biomass May 5th, 2005	$y = -493.9 + 106.8 C_{org\ 0-5} -2.9SIR -192.3C_{LOMabs} + 9512.4 N_{LOMabs}$	0.9682	0.0006
Biomass July 4th, 2005*	$y = 42.4 -78.9C_{mic}/C_{org} + 5100.9 N_{LOMabs} + 31.7PCA4$	0.8884	0.0029
Biomass April 30th, 2006*	$y = 69.6 + 39782 N_{LOMabs}+ 145.8 PCA 4 -9.7SIR - 757.9C_{LOMabs}$	0.9769	0.0003
Growth inventory 1 – 2*	$y = 22.8 +8421.5 N_{LOMabs}+ 27.2 PCA4 -1.8SIR -167.6C_{LOMabs}$	0.9706	0.0005
Growth inventory 2 – 3	$y = 347.4 -56.4C_{org\ 0-5} + 13.9 N_{LOM\%} -19.6P_{LOM\%} -11.1$ decomp0.1	0.9712	0.0005

*Intercept not significant

All variables were significant at α = 0.05. The regression formulated for the first inventory date was exceptional in number and type of parameters. C_{org} – in the form of the single parameter or integrated in PCA component 4 - was represented in all regressions, and so was N_{LOM}. Parameter C_{mic} – as SIR-CO_2-rate, qCO_2 or C_{mic}/C_{org} – entered in all but the exceptional last regression, where average growth was mostly negative. Predicted and observed biomass and growth values are shown in fig.82 for biomass at the inventory of July 4th, 2005 as an example. Coefficient of determination was close to 1 for all biomass and growth data. The graph illustrates, that a disproportionate part of the trend is owed to the good plant performance on subplot 10, but also, that most other points fit very well into this tendency.

For the inventory of July 4th, 2005, and growth between the first two inventory dates, a sensitivity analysis was carried out to assess the impact of the dominant parameters (fig.83). All except one predictor were kept stable at the mean value of all subplots and the remaining variable was varied from 10 – 190% of its average value.
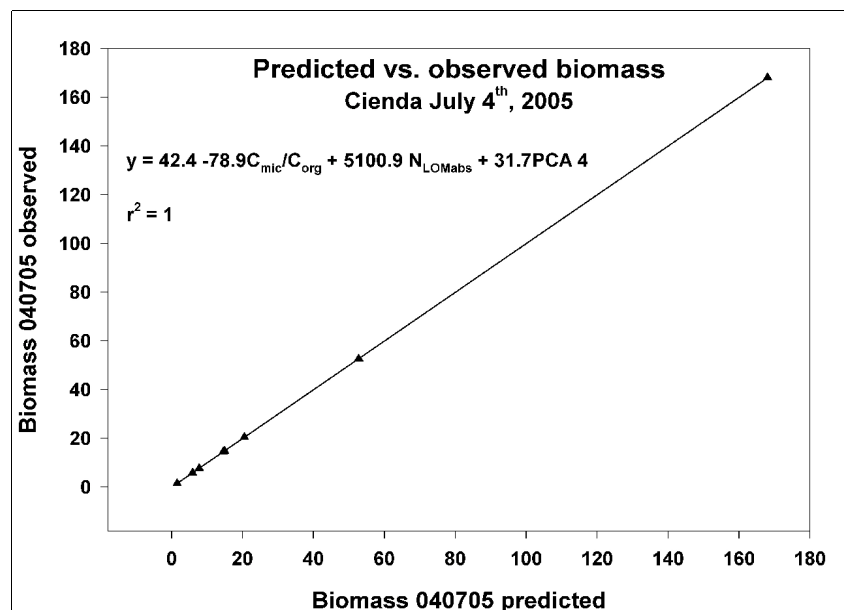

Predicted vs. observed biomass
Cienda July 4th, 2005

$y = 42.4 -78.9C_{mic}/C_{org} + 5100.9 N_{LOMabs} + 31.7PCA 4$

$r^2 = 1$

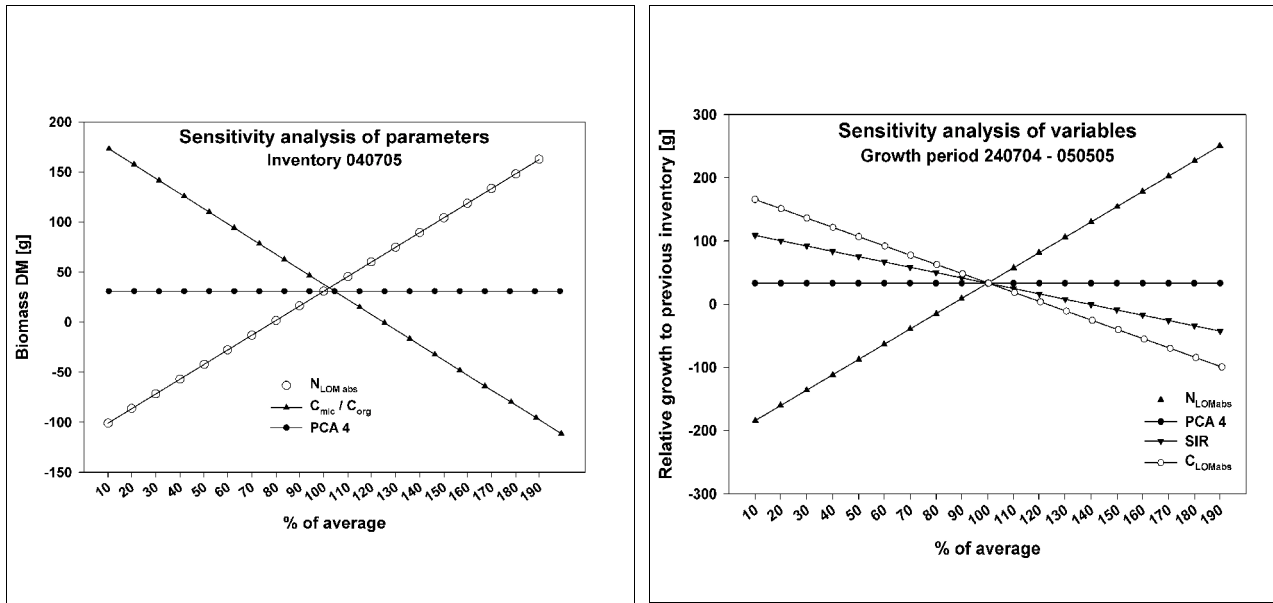*Figure 82: Predicted vs. observed biomass for the 3rd inventory*

Figure 83: Sensitivity analysis of variables for the regressions on growth from July 24th, 2004 to May 5th, 2005, and on biomass at the 3rd inventory (July 4th, 2005).

As recognisable from the steepness of slopes, N_{LOMabs} had the strongest influence on growth, followed by C_{LOMabs} and SIR; PCA 4 was almost horizontal and did not affect growth. At the third inventory, C_{mic}/C_{org} and N_{LOMabs} had similar though opposed impact on biomass, whereas PCA 4 again was not influential. Removing PCA 4, however, led to a drastic reduction of r-square, implying intercorrelations between variables. On the other hand, PCA 4 could be replaced by C_{org}0-5cm without much decrease in fit.

It is known, that banana plants require fertile sites rich in organic matter and of slightly acidic to neutral pH (REHM & ESPIG 1996) and the same has been assumed for abaca as a close relative (KELLMAN 1970). Usually advanced fallows or sites under secondary forest are selected for abaca plantations. For this reason, factors connected to carbon and nitrogen as well as microbial carbon contributed to the fit of equations whereas light-related parameters did not and P only for two of six regressions.

The relevance of the LOM fraction for N availability for plants has been highlighted by ZECH ET AL. (1997). BARRIOS ET AL. (1997) state, that trees have the potential to increase availability of N compared to annuals and the explanatory power of N for the fast-growing abaca plants was confirmed for both sets of equations.

On the other hand, litter and soil organic matter are important for the water holding capacity of soils, so that an effect of water balance cannot be ruled out for any equation.

Each multiple regression presented here is only one of several possibilities to predict biomass/growth from a set of preselected parameters, which is then reduced by the elimination procedure due to the explanatory power of the single factors. In a first approach, some regressions had been formulated for PAR, among others, showing a negative impact of increasing PAR on biomass and growth. Relationship of PAR and biomass / growth was negative at all times, implying that radiation in the observed range was connected to a stress factor. This negative effect of PAR has been discussed before. With respect to the dependent variable *growth 2,* it could be assumed, that stress-related variables would have had a statistical impact on the negative rates. Still, parameters PAR and qCO_2 did not meet the required significance level to remain in the model.

PAR as a single parameter was not coherent with growth. Measurements conducted at

• 157

tree positions (s. 5.1.8) and intrapolated to the corresponding abaca locations were related to the height measurements at each of the five abaca inventories. Direct interrelations, mainly optimum curves, between abaca growth and PAR were calculated, but never of $r^2 > 0.20$.

As shown before, biomass and growth were clearly highest on subplot ten. If subplots are ranked by soil parameters, this subplot was above average for C_{Lol}, C_{LOM} and N_{LOM}. Subplot eight, with the second highest growth rates, ranked last for C_{Lol}, C_{LOM}, N_{LOM} and C_{mic} and first for pH and qCO_2. With respect to qCO_2, subplot 10 was second. With respect to P_{LOM}, both are low in contents compared to the other subplots. This is remarkable as P is frequently assumed to be the most limiting factor for plants on volcanic soils in Leyte. Subplot 2, the supposedly best subplot for planting, if judging from the environmental parameters discussed in 5.1.9, was far behind 8 and 10.

Interestingly, banana had been traditionally planted to greater extent only on the two subplots, that proved to be best for growth, namely 8 and 10. It would be worthwhile to investigate farmers' criteria and site indicators for planting banana and abaca. Two contrasting possibilities are that, a.) farmers have an empiric knowledge on additional factors which were not considered in this study and which benefit abaca/banana growth especially on sites with the lowest fertility, or b.) banana has always been planted on these spots and will be grown there as long as soil fertility allows it. The good performance at some spots would then be attributable to more regular weeding on the traditional banana land.